Chapter 2

Literature review of zinc oxide (ZnO) nanostructures

2.1 Introduction

In this chapter a literature review on zinc oxide (ZnO) nanostructures will be presented in detailed. Implications of nanotechnology in general, its definitions, emergence and its history are explained in section 2.2. Nanomaterials and their classification will be summarized in sections 2.3 and 2.4 respectively. Nano-electromechanical system is described in section 2.5. Descriptions of zinc oxide including; crystal structure, properties, doping and applications are outlined in section 2.6. Review of different growth techniques that have been used in ZnO nanofabrications is presented in section 2.7. Overview discussions and some previous results from the literature on the effect of different growth parameters on the growth process are outlined in section 2.8. In section 2.9, a review of different growth mechanisms that have been suggested to explain the growth process of nanostructures is discussed in detailes. Finally, descriptions of various characterization techniques that have been used in this study are illustrated in section 2.10.

2.2 Nanotechnology

Nanotechnology is a general term that even the scientists do not have a general consensus on the meaning of the word. There are many definitions that scientists working in nanotechnology use. These definitions are true for certain specific research fields, but none of them covers the full spectrum of nanotechnology. In the United States, working group on nanoscience, engineering and technology has been defined that nanotechnology is "concerned with materials and systems whose structures and components exhibit novel and significantly improved physical, chemical and biological properties, phenomena and processes due to their nanoscale size" [18]. In addition, it is good to point out another further definition of nanotechnology to date appears on the NASA website which is the most widely accepted in this field. The definition appears as follow: "The creation of functional materials, devices and systems through control of matter on the nanometer length scale (1-100 nanometers), and exploitation of novel phenomena and properties (physical, chemical, biological) at that length scale" [19]. Recently, another definition of nanotechnology by the Environmental Protection Agency (EPA) in their 2007 Nanotechnology Whitepaper has been emerging. EPA defines nanotechnology as: “research and technology development at the atomic, molecular, or macromolecular levels using a length scale of approximately one to one hundred nanometers in any dimension; the creation and use of structures, devices and systems that have novel properties and functions because of their small size; and the ability to control or manipulate matter on an atomic scale” [20]. As a result, nanotechnology is not exclusive to only one field. There are many fields contributed to nanotechnology, including molecular physics, materials science, chemistry, biology, computer science, electrical engineering and mechanical engineering. In general, nanotechnology covers a technology of design, fabrication and applications of nanostructures and nanomaterials to produce novel devices that have useful and unique properties.

The emergence of nanotechnology is not new at all, and some of nanomaterials are around us as well as inside our bodies. For examples, Chinese were known to use Au nanoparticles as an inorganic dye to introduce red color into their ceramic porcelains more than thousand years ago as shown in Fig 2.1(a) and (b) [21]. Use of colloidal gold has a long history, though a comprehensive study on the preparation and properties of colloidal gold was first published in the middle of the 19th century [22]. Colloidal dispersion of gold prepared by Faraday in 1857, [23] was stable for almost a century before being destroyed during World War II [22]. Medical applications of colloidal gold present another example. Colloidal gold was, and is still, used for treatment of arthritis. A number of diseases were diagnosed by the interaction of colloidal gold with spinal fluids obtained from the patient [24]. Moreover, nanotechnology is also around us. It has been discovered that a type of bacteria, called "magnetotactic bacteria", has evolved an ingenious method of navigation via magnetic nanoparticles lined up inside the organism, acted on by the earth's magnetic poles (illustrated in Fig. 2.1(c)). While cells and bacteria are often relatively large compared to viral dimensions. The viral dimensions are well within the nano-regime, allowing them to easily be transported throughout the body, and even into cell interiors as illustrated in Fig. 2.1(d).

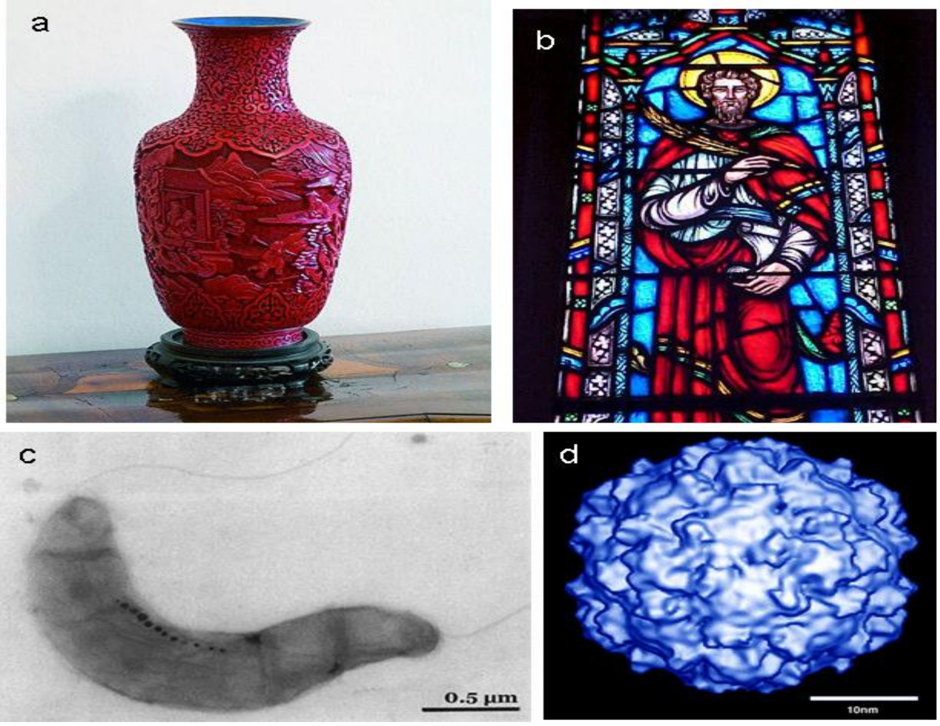

Fig. 2.1. (a) an 18th century Chinese vase, demonstrating use of red glaze pigments (b) a medieval stained glass window illustrating use of nanopowders in art glass processing (c) a magnetotatic bacteria, with internal magnetic nanoparticles clearly visible (d) a to-scale computer model of the polio virus [25].

The root of nanotechnology can be traced back to1959. In a talk given by a famous physicist, Richard Feynman, he suggested a process by which the ability to manipulate individual atoms and molecules might be developed, using one set of precise tools to build and operate another proportionally smaller set, and so on, down to the needed scale. After that, in 1974 the term "nanotechnology" was first used by Professor Norio Taniguchi. He described it as*: "Nano-technology' mainly consists of the processing of, separation, consolidation, and deformation of materials by one atom or by one molecule* [26]".

In fact, the development of the requisite tools began in early 20th century. The first electron of a prototype microscope, based on fundamental scientific discoveries by physicist Loius de Broglie, was developed in 1931 by Ernst Ruska and colleagues. Improvements in both the scanning and transmission electron microscopy soon followed. Very recently, the equipment which named as Super STEM 2 is capable of imaging at the resolution of over more than 20 million times [27]. These developments have provided scientists the ability to probe material composition down to individual atoms. With these powerful tools, scientists can investigate structures and identify changes in materials that were previously impossible.

2.3 Nanomaterials

Nanomaterials are not just very small. They also exhibit high performance and novel properties than their bulk structures. For example, the optical properties of CdSe nanoparticles are related with their size as shown in Fig. 2.2 [28]. The optical emission of CdSe nanopartials is size dependent. In quantum mechanics, as particles become smaller (the quantum well gets deeper) the possible energy levels are shifted upward to higher energies. These energy shifts can be observed as the changes in optical emission in a quantum dot, since photons emitted from a material have frequencies directly related to the separation between the electron energy bands of the material [29].

Fig. 2.2. Vials containing varying sizes of CdSe quantum dots, growing larger from left to right [28].

In addition, the physical and chemical properties change dramatically as material size reaches nanosize. Platinum nanoparticles melted at temperatures far below the melting point of the bulk metal. This is an example of the changing of physical properties as the size decreases. Carbon nanotubes have been shown to have unique properties. Their stiffness and strength are higher than any other material. They also have extraordinary electronic properties. Carbon nanotubes (CNTs) are reported to be thermally stable in vacuum up to 2800 degrees centigrade, to have a capacity to carry an electric current a thousand times better than copper wires, and to have twice the thermal conductivity of diamond (which is another form of carbon). Furthermore, it was found that depending on the chirality of the atomic arrangements, carbon nanotubes could exhibit either semiconducting or metallic electron transport. CNTs in the “zig-zag” [30] conformation, demonstrate semiconductor-like electronic conduction in which a band gap must be overcome to free transport electrons, while “armchair” [30] CNTs behave similar to metals as shown in Fig. 2.3.

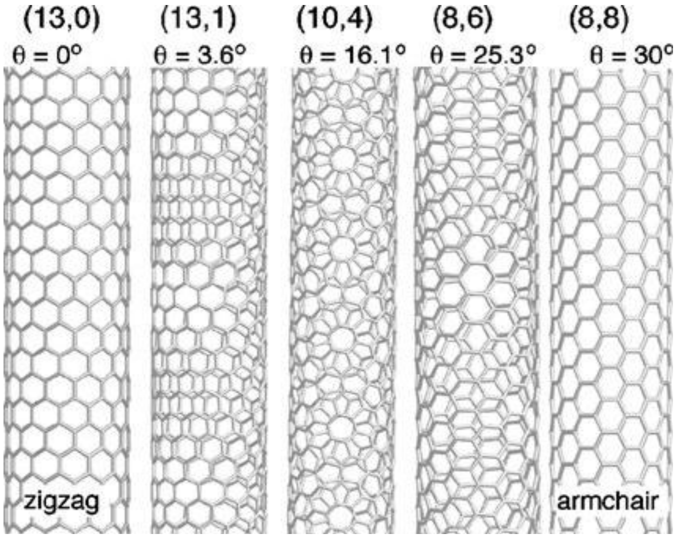

Fig. 2.3. Computer generated structures of single-wall carbon nanotubes with different chiral angles between 0° and 30°[30].

2.4 Classification of nanomaterials

According to their dimensionalities, nanomaterials are commonly classified as zero dimensional (0D) (quantum dots or mostly spherical nanoparticles), one dimensional (1D) (nanowires, nanotubes, and nanobelts), two-dimensional (2D) (thin films and quantum wells) and three-dimensional (3D) (plates and flower-like) as shown in Fig. 2.4. The classification is based on the number of dimensions in which the material is outside the nano- regime. A thin film, for example, consists of large expanses of material in both in-plane directions, and is nanosized only in its thickness; therefore it is termed a two-dimensional (2D) nanomaterial. Due to the effects of size discussed in the previous section, the dimensionality of a nanomaterials can alter their properties. A thin film may behave very differently from a nanowire with the same chemistry. These distinctions therefore are not arbitrary, but important in distinguishing these materials according to their unique characteristics.

0 D	**1D**	**2D**	**3D**
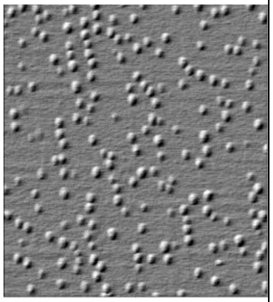	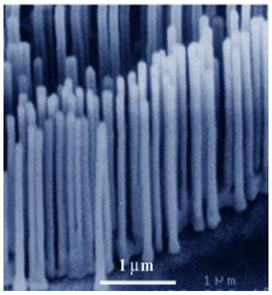	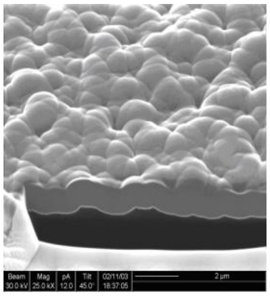	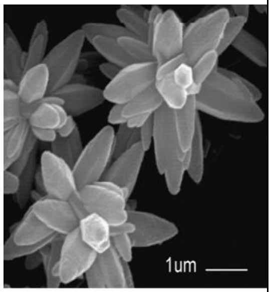
Quantum Dots	Nanowires	Thin Films	Nanoflower-like

Fig. 2.4. Images demonstrating nanomaterial classifications.

2.5 Nano-electromechanical systems (NEMS)

In specify time, we had Micro-Electro-Mechanical Systems (MEMS) that were integrally fabricated from hybrids of micromechanical and microelectronic elements. As the science and technology advanced, Micro-Electro-Mechanical Systems (MEMS) became much smaller and shrinking in thickness and width to nanosize. This is the guide to evolve the Nano-Electro-Mechanical Systems (NEMS) with new scientific studies and technical applications. The small mass and size of NEMS give them a number of unique attributes that offer immense potential for new applications and fundamental measurements. For example, as mechanical devices became smaller, their novel properties raised. For example, the increase in the resonant frequency, the lowering of the force constants and the dissipation only little energy, are shown in smaller NEMS. Obviously, it is remarkable that the computer industry has successfully pushed sharply for more powerful and high speeds as well as, smaller devices.

According to “Moore’s Law,” a prediction that the number of transistors on an integrated circuit could grow by a factor of 2 approximately every 18 months – industry leaders have acknowledged that soon the expansion will slow due to the physical limits of miniaturization as illustrated Fig. 2.5. Until today, the best microchips contain millions of transistors whose critical dimensions measured only 100 atoms across [31]. However, the commercial market for nanotechnology products is estimated to reach $29 billion by the end of 2008 [32]. The recent acceleration of marketable nanotech products and ideas is made evident through the last decade’s surge in nanomaterials patents. As of January 2008, the US Patent Office had awarded approximately 2800 nanoscience patents. In perspective, consider that the number of patents containing the phrase “nano” numbered only 70 in 1990 and 800 by 2001 [33]. Forecasters predict that the next 10 years will experience an even greater boom of nanomaterials enabled products. Commonly, medicine, electronics, energy, and defense are cited as some of the most promising fields for these new technologies.

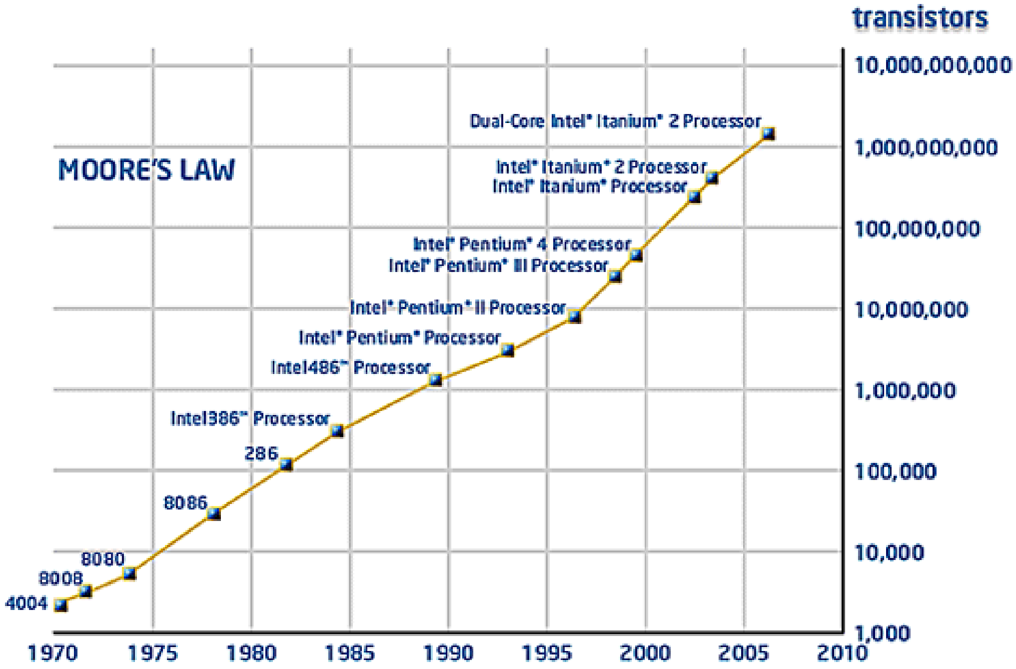

Fig. 2.5. A graph of the exponential growth of IC transistors according to Moore's Law from 1971 to 2000.

However, researchers in the field face many new challenges that are unique to nanostructures and nanomaterials. In many cases, synthesis of nanostructures is not well understood, so that scientists must repeat attempts several times to achieve desired products. Such obstacles make these materials slow to produce, very expensive, and resistant to scale-up processing required for commercial manufacture. Nanomaterial properties are strongly correlated to their geometry and dimensions. Therefore, precise control over synthesis is required to create high quality and consistent products. Often localization to a certain location in a device requires many trials and high percentages of wasted material. The small size and complexity of nanoscale structures make the development of new measurement technologies more challenging than ever. New measurement techniques need to be developed at the nanometer scale and may require new innovations in metrological technology. For example, measurements of physical properties of nanomaterials require extremely sensitive instrumentation and the noise level must be kept very low.

2.6 Zinc oxide

Zinc oxide (ZnO) is a white or yellowish powder as shown in Fig 2.6. It has the molecular weight of 81.37, average atomic weight of 40.69amu and enthalpy of formation (298.15K) of 350.5 kJ/mol. There are two main processes for commercially producing powdered ZnO. In first method, which is called direct or American process, zinc ores are heated in the air with coke or anthracite. This gives zinc vapor which is subjected to controlled oxidation. In the second method, which is named indirect or French process, where the zinc vapor is obtained by boiling zinc which then, subjected to controlled oxidation. Nowadays, ZnO has attracted intensive research effort for its versatile applications and it exhibits many unique interesting properties. In this section, a discussion of the most important zinc oxide properties will be presented in details.

Fig 2.6. Zinc oxide powder.

2.6.1 Crystal structure of zinc oxide

ZnO is one of II-VI compound semiconductors. It has crystal structure of wurzite (hexagonal symmetry), zinc blends or rock salt (cubic symmetry) as shown in Fig. 2.7. However, ZnO crystals most commonly stabilize in the wurzite structure with a hexagonal unit cell (space group *P63mc*). The crystals exhibit the rock salt phase only at high pressures.

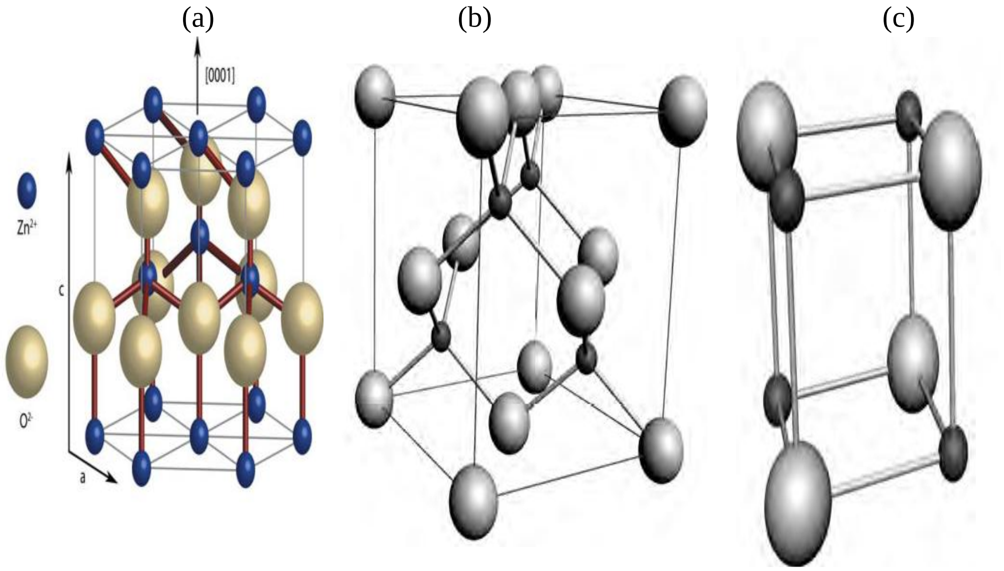

Fig. 2.7. Different ZnO crystal structures (a) wurzite, (b) zinc blend and (c) rock salt.

The wurtzite structure of ZnO can be considered to be composed of two interpenetrating hexagonal close packed (hcp) sublattices of cation (Zn) and anion (O) displaced by the length of cation-anion bond in the c-direction. The lattice constants of the ZnO hexagonal unit cell are a=3.2500 Å and c=5.2060 Å at 300K. The c/a ratio for ZnO is 1.60 which is close to the 1.633 ratio of an ideal hexagonal close-packed structure. Each hexagonal close packed (hcp) consists of one type of atom displaced with respect to each other along the threefold c-axis by the amount of u =3/8 = 0.375 in fractional coordinates (the u parameter is defined as the length of the bond parallel to the c axis, in units of c or nearest neighbor distance b divided c).α and β are the bond angle 109.070 as shown in Fig. 2.8.

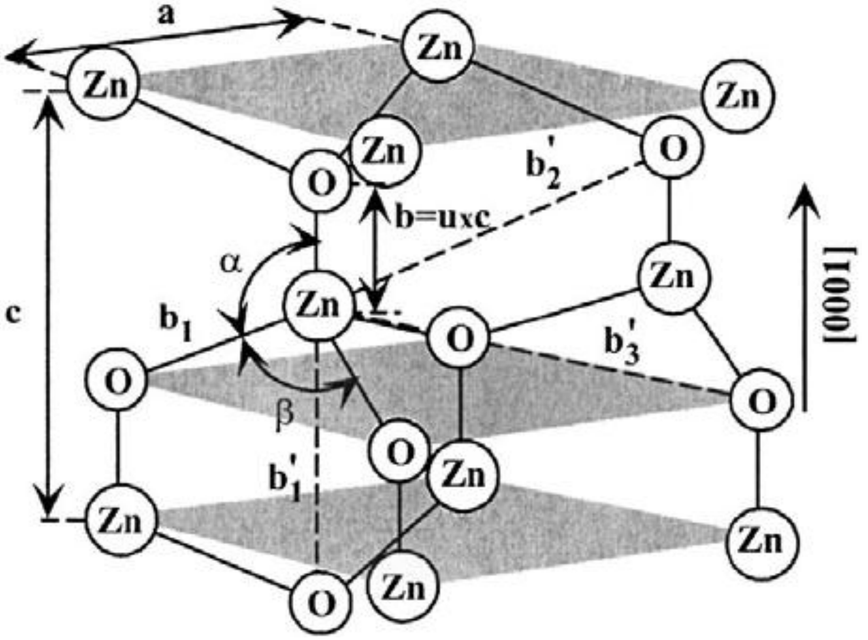

Fig. 2.8. A schematic diagram of a wurtzitic ZnO structure [34].

In such structure each anion is surrounded by four cations at the corner of tetrahedron and vice versa. The bonding in these materials are usually (sp3) covalent (tetrahedral) but some ionic characteristics have been found in these material as well. In a real ZnO crystal, the wurtzite structure deviates from the ideal arrangement, by changing the c/a ratio or the u value. The deviation from that of the ideal wurtzite crystal is probably due to lattice stability and ionicity. The point defects such as zinc antisites, oxygen vacancies, and extended defects, such as threading dislocations also increase the lattice constant in ZnO crystal, but for a small extent in hetero-epitaxial layers. There exists a strong relationship between the c/a ratio and the u parameter in that when the c/a ratio decreases, the u parameter increases in such a way that those four tetrahedral distances remain nearly constant through a distortion of tetrahedral angles due to long-range polar interactions.

2.6.2 Physical properties of wurtzite zinc oxide

The investigation and understanding of the fundamental physical properties of ZnO are important for many reasons. For example, they are helpful to the rational design of functional devices and for developing their potential as the building blocks for future nanoscale devices. Table 2.1 shows a compilation of the basic physical parameter for bulk ZnO. It is worth to note that there is still some uncertainty in these values. For example, a few reports have mentioned the physical properties of only p-type ZnO and therefore, the hole mobility and effective mass are still in debates [34,35]. In addition, as the dimension of the semiconductor materials continuously shrinks down to nanometer or even smaller scale, some of their physical properties undergo changes known as the “quantum size effects”. The quantum confinement increases the band gap of ZnO nanowires, which has been confirmed by photoluminescence measurements [36,37].

Table 2.1. Physical properties of wurtzite ZnO [38]

Property	**Value**
Lattice parameters at 300 K	
a_0	0.324 95 nm
c_0	0.520 69 nm
a_0/c_0	1.602 (ideal hexagonal structure shows 1.633)
u	0.345
Density	5.606 g cm^{-3}
Stable phase at 300 K	Wurtzite
Bond length	1.977 Å
Melting point	1975 ◦C
Thermal conductivity	0.6, 1–1.2 Wcm^{-1} K^{-1}
Linear expansion coefficient	a_0: 6.5 × 10^{-6} (C^{-1}) c_0:3.9 x 10^{-6} (C^{-1})
Static dielectric constant	8.656
Refractive index	2.008, 2.029
Energy gap	3.4 eV, direct
Intrinsic carrier concentration	<10^6 cm^{-3}
Breakdown voltage	5.0 × 10^6 V cm^{-1}
Saturation velocity	3.0 ×10^7 cms^{-1}
Exciton binding energy	60 meV
Electron effective mass	0.24 m_0
Electron Hall mobility at 300 K for low n-type conductivity	200 cm^2 $(V s)^{-1}$
Hole effective mass	0.59 m_0
Hole Hall mobility at 300 K for low p-type conductivity	5–50 cm^2 $(V s)^{-1}$
Knoop hardness	0.5N/cm^2
Bulk hardness, *H*	5.0±0.1 GPa
Minimum pressure at melting point	7.82atm
Ionicity	62%
Heat capacity C_p	9.6 cal/molK
Heat of crystallization ΔH_{ls}	62KJ/mol
Young’s modulus E (bulk ZnO)	111.2±4.7 GPa
Bulk modulus, B (Polycrystalline ZnO)	142.2 Gpa
dB/dP	3.6
Spontaneous polarization	-0.057 (C/m^2)
Born effective charge	2.10

2.6.2.1 Mechanical properties

Direct measurement of the mechanical properties of individual ZnO nanostructures is really challenging. Thus, there are very few experimental investigations on mechanical properties of ZnO nanostructures. In fact, the lack of the experimental studies for ZnO nanostructures is mainly attributed to some challenges that come out from the characterization techniques of nanoscaled material, such as (i) specimen manipulation, alignment and gripping to achieve the desired boundary conditions, and (ii) application and measurement of force and displacement with very high resolution [39]. According to Table 2.1, ZnO is a relatively soft material, with a hardness of 5 GPa at a plastic penetration depth of 300 nm (for c-axis oriented bulk ZnO). Some researchers tried various techniques to measure the Young's modulus of ZnO nanostructures. Based on an electric-field-induced resonant excitation, Bai et al. characterized the bending modulus of ZnO nanobelts using Transmission Electron Microscope (TEM) [40]. In this method, a special TEM sample holder was made to apply an oscillating electric field between a ZnO nanobelt and a fixed electrode. This electric field drove the vibration of the nanobelt, and resonant oscillation was achieved by tuning the driving frequency. Following the classical elasticity theory, bending modulus was calculated and it was found to be 50 GPa. In addition, Atomic Force Microscope (AFM) based experiments are popular techniques for mechanical characterization of ZnO nanostructures. Because the stiffness of the AFM tip is very small, the force measurement resolution is very high (nano-Newtons). In this technique, very soft spring (e.g. cantilever beam) was used to bend the ZnO nanowire. Song et al. [41] and Hoffman et al. [42] have used this technique to measure the Young's modulus of ZnO nanowires. They reported different values of Young's modulus of 29 ± 8 and 97

±18 GPa respectively. At the bulk scale, the Young's modulus of zinc oxide in the [0001] direction is 140 GPa [43], which is significantly higher than the modulus value reported for ZnO nanostructures.

2.6.2.2 Electrical properties

Due the novel electrical properties, ZnO is representing a lot of attraction for optoelectronic and electronic devices. For example, a device made from ZnO material have a high breakdown voltage, lower noise generation, and can operate at higher temperatures with high operation power. The background carrier concentration of ZnO is usually 10^{16} cm^{-3} and the electron effective mass of ZnO is $0.24m_o$ (m_o being the free electron mass), while the hole effective mass is $0.59m_o$ [38]. In addition, electrical transport studies after configuring individual ZnO nanowires as field effect transistors (FET) confirm that as-grown ZnO nanowires exhibit n-type behavior [44]. Typically the field-effect mobility of as-grown nanowires is in the range of 20–100 cm^2/V s [45]. Later, Park *et al*.[46] have reported an electron mobility of 1000 cm^2/V s after coating the nanowires with polyimide passivation layer to reduce the electron scattering and trapping at surface. Recently, it has been discovered that after coating the ZnO nanowire with a layer of SiO_2 followed by Si_3N_4 to passivate the surface states, the mobility of ZnO nanowires can be dramatically enhanced to exceed 4000 cm^2/V s [47]. These results indicate that the ZnO nanostructures based devices have exceptional potential in high speed electronics application.

2.6.2.3 Optical properties

The optical properties of ZnO nanostructures have been extensively studied because of their promising potentials in optoelectronics. The optical properties of ZnO nanostructures are associated with both intrinsic and extrinsic effects. Intrinsic optical transitions take place between the electrons in the conduction band and holes in the valence band, including excitonic effects due to the Coulomb interaction. Extrinsic properties are related to dopants or defects, which usually create discrete electronic states in the band gap, and therefore influence both optical-absorption and emission processes. ZnO tends to intrinsically form as an n-type semiconductor material, in which the electrical conductivity is due to excess zinc, presumably interstitially within the lattice and to oxygen vacancies [48]. Extrinsic defects such as hydrogen are more likely to be incorporated as shallow donors [49]. In general, ZnO is wide direct semiconducting band gab (3.4 eV) and this makes it potentially useful for efficient UV laser diodes (LDs) and low power thresholds for pumping at room temperature. It is also one of the promising materials in high temperature and high power devices. A high temperature operation requires a wide band-gap so that the intrinsic carrier concentration remains. A high power operation is attractive for wide band gap semiconductors due its higher breakdown fields.

Experimentally, photoluminescence (PL) spectra of ZnO nanostructures have been broadly reported. Room temperature PL spectrum of ZnO is usually composed of a near UV-emission band (380 nm) due to band-to-band transition and a green-yellow emission band related to oxygen vacancy [50]. In addition, red emission band was also reported and it was attributed to doubly ionized oxygen vacancies [51]. It has been reported that the green emission intensity of ZnO is increased with decreasing nanowires diameter. This suggested that the defect level was higher in thinner nanowires due to the increasing surface-to-volume ratio. Continuous reduction of the diameter of ZnO nanowire results in a quantum size effect which manifests itself in the blue shift of band-edge emission in the photoluminescence spectra (as demonstrated in Fig. 2.9) [37].

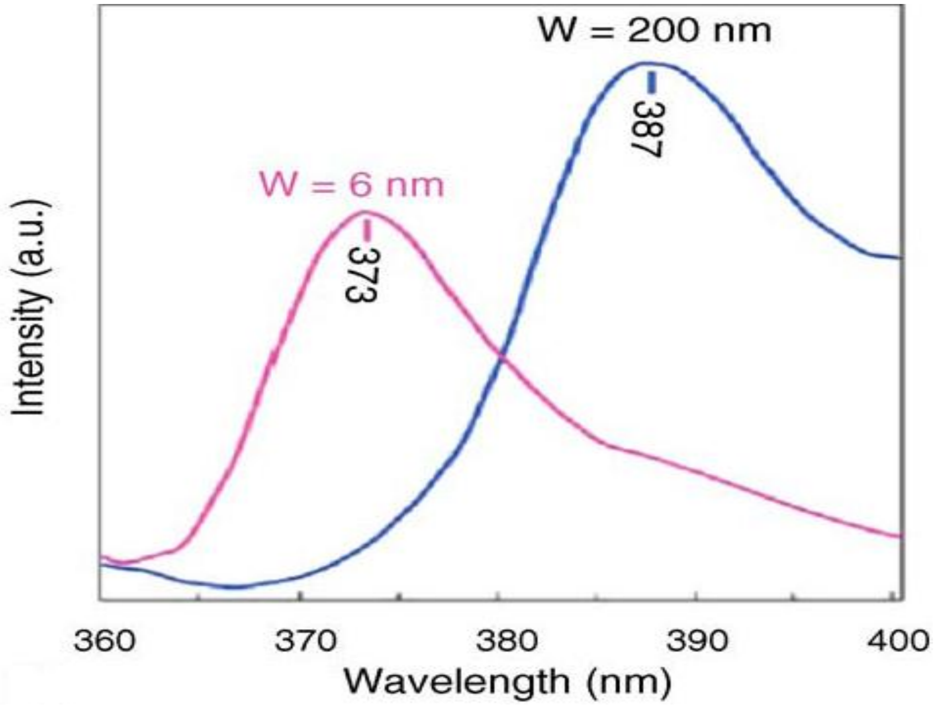

Fig. 2.9. PL spectra of 6 nm and 200 nm wide ZnO nanobelts showing a blue shift of the emission peak [37].

In addition, the most important advantage of ZnO nanostructures is the high exciton binding energy (60 meV), which is 2.4 times the effective thermal energy (K_{BT}=25meV) at room temperature, giving rise to efficient exitonic emission at room temperature. This is one of the key parameters that ZnO exhibits lasing emission at room temperature. The additional advantages of ZnO nanowire lasers are that the excitonic recombination lowers the threshold of lasing, and quantum confinement yields a substantial density of states at the band edges and enhances radiative efficiency. Moreover, due to its near-cylindrical geometry and large refractive index (~2.0), ZnO nanostructures are a natural candidate for optical waveguides [52].

2.6.3 Doping of zinc oxide

Doping of a semiconductor is defined as the addition of a small percentage of foreign atoms in its regular crystal lattice with the intent of producing dramatic changes in electrical, optical, and magnetic properties, which is important for practical applications. As a wide band gap semiconductor, ZnO is gaining much importance for the possible application due to the capability of ultraviolet lasing at room temperature and possibilities to engineer the band gap. In order to attain the potential offered by ZnO, both high-quality n- and p-type ZnO are essential.

2.6.3.1 *N*-type doping

As grown, ZnO nanostructures are n-type due to structural defects from the growth process, such as oxygen vacancies, zinc interstitials and antisites. An antisite occurs when a nucleus of one species occupies a lattice site that is typically occupied by another species, such as a zinc atom on an oxygen site. A vacancy is an unoccupied lattice site, resulting in unsatisfied bonds within the lattice. An interstitial defect is formed by an interstitial atom that does not occupy a lattice site. Photoluminescence and temperature dependent Hall studies of electron irradiated ZnO have shown that Zn is the most likely candidate for purely lattice-related dominant shallow donor, with an activation energy about 30-50 meV [53]. There is another assumption that the n-type conductivity of ZnO nanostructures is due to hydrogen (H), which is treated as a shallow donor with activation energy of 30 meV instead of Zn. This assumption is valid because hydrogen (H) is always present in all growth methods and can easily diffuse into ZnO in large amounts due to its large mobility [54]. This suggestion is based on the fact that hydrogen is present in almost all growth technique relative to ZnO. This assumption has been shown that hydrogen with activation energy 39 meV acts as main donor during seeded chemical vapor transport (SCVT) growth of ZnO. This donor disappears through on annealing process [55]. Controllable n-type doping is easily achieved by substituting Zn with group-III elements Al, Ga, In or by substituting oxygen with group-VII elements chlorine or iodine. The n-type ZnO doping is resulting in high-quality, highly conductive such as Al-doped ZnO had shown a high conductivity with low resistivity [53].

2.6.3.2 *P*-type doping

It is very difficult to obtain p-type doping in ZnO. Oxygen interstitial O_i and zinc vacancy V_{zn} are believed to create deep impurity levels which cause large resistance. The *p*-type doping in ZnO may be possible by substituting either group-I elements (Li, Na, and K) for Zn sites or group-V elements (N, P, and As) on O sites. It was found that group-I elements could be better *p*-type dopants than group-V elements in terms of shallowness of acceptor levels [34]. However, group-I elements tend to occupy the interstitial sites, due to their small atomic radii, rather than substitutional sites, and therefore, they act as donors instead of acceptors. Moreover, larger bond length for Na and K than ideal Zn–O bond length (1.93 Å) induces lattice strain, increasingly forming native defects such as vacancies which compensate the shallow dopants. These are among the many causes leading to difficulties in attaining *p*-type doping in ZnO [56, 57]. On the other hand, both P and As belong to group V elements, have a larger bonds lengths. Therefore, they are likely to form antisites to avoid the lattice strain. Of the possible acceptor species for ZnO, nitrogen is the favorite because the Zn-N bond (1.88 A) is the most similar in length of the Zn-O bond (1.93 A) as illustrated in Table 2.2. Close matching of the bond length reduces the crystal strain and thus, reduces the likelihood of compensating defect formation. For this reason, it is preferable to develop methods of doping ZnO nanostructures with nitrogen.

Table 2.2 Group I and V acceptor properties in ZnO [56]

Dopant	Bond length (A)	Calculated energy level (meV)	Group
Li	2.03	90	I
Na	2.10	170	I
K	2.42	320	I
N	1.88	400	V
P	2.18	930	V
As	2.23	1150	V

2.6.4 Some applications of zinc oxide

ZnO is a very important material and it has attracted intensive research effort for its unique interesting properties such as anisotropy in the crystal structure, nonstoichiometric defect structures, high exiton binding energy, wide band gap, optical transparency in the visible light, high refractive indices, large piezoelectric constants, and nonlinear optical coefficient. Due these novel properties, ZnO has been used for acoustic wave devices, gas sensors, piezoelectric transducers, light emitting diodes (LEDs) and laser diodes (LDs) transparent electrodes [58]. In fact, the predominant material for blue or UV light emitting diodes (LEDs) is gallium nitride (GaN). However, ZnO nanostructures are promising candidates for nanoelectronic and nanophotonics devices. ZnO has several fundamental advantages over GaN; (i) its free exciton (60 meV) is much higher than that of GaN (21–25 meV); (ii) it has a high energy radiation stability, making it suitable candidate for space applications; (iii) it has more amenability to wet chemical etching and it can be grown in native substrate [59], ZnO is also a candidate for blue to UV optoelectronics, including lasers which has important applications in high density data storage systems, solid-state lighting (where white light is obtained from phosphors excited by blue or UV light-emitting diodes), secure communications and bio-detection [56]. In addition, zinc oxide has been used in a variety of technical applications, including porcelain enamels, heat resisting glass, an activator in vulcanization, an additive for rubber and plastics, pigment in paints with UV-protective and fungi static properties, spacecraft protective coatings, a constituent of cigarette filters, healing ointments and in optical waveguide [34]. Recently, based on piezoelectricity effect of ZnO nanowires, nanogenerator driven by an ultrasonic wave was achieved [60] as shown in Fig. 2.10. Finally, it is worthy to note that ZnO has been also used in medical applications such as sunburn prevention, nappy rash, skin irritations, cold sores, cuts and burns treatments.

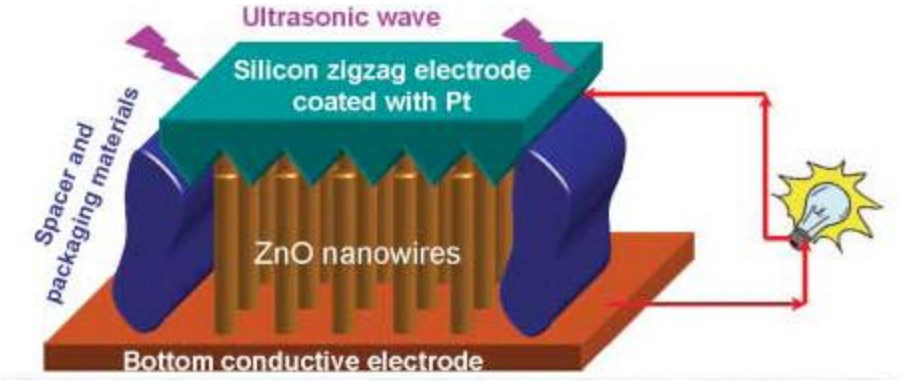

Fig. 2.10. A schematic diagram of the design and structure of the nanogenerator based on ZnO nanowires [60].

2.7 Fabrication of nanosized of zinc oxide

There are two major methods used in the synthesis and fabrication of ZnO nanostructures. These techniques are called top-down and bottom-up. Top-down technique refers to a manufacturing technique whereby an object is created by carefully removing pieces of a larger object-essentially carving out the desired object. In this technique, it is started with a bulk material and then it is broken into smaller pieces using mechanical, chemical or other form of energy. The top-down approach often uses the traditional workshop or micro-fabrication methods where externally-controlled tools are used to cut, mill and shape materials into the desired shape and order. A key advantage of the top-down approach is that the parts are both patterned and built in place, so that no assembly step is needed. The bottom-up approach, or sometimes called self-assembly approaches used chemical or physical forces operating at the nanoscale to assemble basic units into larger structures. In contrast to top-down technique, bottom-up technique starts with small structures and ends with large units.

2.7.1 Ball milling

Ball milling technique is an example of top-down techniques and it has been utilized to produce nano-composites and to ascertain the fundamental parameters of the mechanochemical reaction and the mechanical alloying process. It can also be used to produce alloys, which are ultimately more useful than individual elements because composite alloys are more homogenous than metals and are less corrosive, and have higher melting points and hardness. In fact, ball milling technique is more environmentally safe than the current method of chemical synthesis, producing far less chemical waste. On the other hand, ZnO nanoparticles produced by attrition have a relatively broad size distribution and varied particle shape or geometry. In addition, they may contain a significant amount of impurities from the milling medium and defects resulting from milling.

2.7.2 Solution-based chemistry (SBC)

Solution-based chemistry (SBC) is defined by any chemical reaction that requires a liquid. As a generic method for synthesis, SBC has been vital to the production of a diversity of materials that are often difficult to make using other methods. Typically, solution-based methodologies are of low cost and also provide control materials with high yield and uniformity. However, the growth is complicated and many defects are formed during the reaction. The most important and common techniques for ZnO synthesis are hydrothermal and sol-gel synthesis, both them will be discussed below.

2.7.2.1 Sol-gel synthesis

The sol-gel technique is a long-established industrial process for the generation of colloidal nanoparticles from liquid phase, which has been further developed in last years for the production of advanced nanomaterials and coatings. Sol-gel processes are well adapted for oxide nanoparticles and composites nanopowders synthesis. The main advantages of sol-gel techniques for the preparation of materials are low temperature of processing, versatility, and flexible technology allowing easy shaping and embedding. Sol–gel method has been utilized to obtain ZnO [61] by soaking anodized aluminum oxide (AAO) into zinc nitrate solution mixed with urea and kept at 80°C for 24–48 hours followed by thermal heating.

2.7.2.2 Hydrothermal synthesis

Hydrothermal process has been carried out to produce crystalline structures since the 1970s. As defined, hydrothermal synthesis is a subset of solvothermal synthesis which involves water at elevated conditions. The basic principle is that small crystals will homogeneously nucleate and grow from solution when subjected to high temperatures and pressures conditions. Typically, the temperature ranges between 100 °C and 300 °C and the pressure exceeds 1 atm are used. During the nucleation and growth processes, water is both a catalyst and occasionally a solid-state phase component. Under the extreme conditions of the synthesis vessel, water often becomes supercritical, thereby increasing the dissolving power, diffusivity, and mass transport of the liquid by reducing its viscosity. In addition, the ability to tune the pressure of the vessel provides an avenue to tailor the density of the final product. When compared to other methodologies, hydrothermal synthesis is environmentally benign, inexpensive, and allows for the reduction of free energies for various equilibria. Many studies have been reported to synthesize ZnO nanorods by using wet-chemical hydrothermal approaches [62,63].

2.7.3 Vapor phase transport synthesis

Vapor phase transport (VPT) is an atomic deposition process in which material physically or chemically vaporized from a solid source and transported onto a substrate where it condenses and deposits. According to the approaches of source vaporization, VPT can be in the form of thermal evaporation (by heat), laser ablation (by photons) and sputtering (by positive ions, or electron beam).

2.7.3.1 Thermal evaporation

Thermal evaporation is one of the simplest methods available to synthesize ZnO nanostructures. During this method, the substrate, crucible, and source material are placed inside a vacuum chamber at room temperature. A vacuum is required to increase the vapor pressure during sublimation and often ranges between 10^{-2} and 10^{-9} Torr (ultra high vacuum). Once the vacuum chamber has stabilized at the appropriate pressure, a heating source is used to heat the source material within the crucible to its vapor point. Upon evaporation, the material will re-deposit along the cooler surfaces of the vacuum chambers, as well as the collection substrate. Typical heating sources include radio-frequency (RF) inductive, electron-beam and resistive heating. During electron-beam evaporation, an electron source is aimed at the source material causing localized heating. In comparison, RF induction uses an AC power supply to produce an alternating current through an induction coil. The alternating current generates a magnetic field within the coil. When the source material is placed inside the coil, the magnetic field induces eddy currents within the source material providing localized heat. Although higher frequencies equate to higher heat rates, lower frequencies are better suited for thicker samples. Finally, resistive heating provides heat by sending a high current source through a resistive coil, such as tungsten, and is a non-localized heat source and therefore commonly used for furnace applications. Yao et. al [7], reported a synthesis of ZnO nanobelts using thermal evaporation method.

2.7.3.2 Sputtering

Sputtering is the removal of surface atoms using high energy ions. There are four common types of sputtering, namely, focused ion-beam, direct current (DC), radio-frequency (RF), and magnetron. In focused ion-beam sputtering, ions are accelerated through a vacuum towards a sample surface. Acceleration and focusing capabilities are provided by a series of capacitive plates and magnetic coils, respectively. In DC sputtering, the substrate and source material are placed inside a vacuum chamber. Upon evacuation of foreign gases, an inert gas, such as argon, is introduced into the chamber at low pressures. Then, a DC power supply is used to ionize the inert gas in order to produce charged plasma. The ions are accelerated towards the surface of the target, causing atoms of the source material to break off from the target and condense on all surfaces including the substrate. A limitation of DC sputtering is that it requires a high voltage to sputter insulating materials, especially when there is a build-up of positive charge on the target material. To solve this problem, the DC power source is often replaced by an RF power source. In addition, to increase the deposition rate, a strong magnetic field (magnetron sputtering) can be used to concentrate the plasma near the substrate.

2.7.2.3 Laser ablation deposition

Laser ablation, a method that combines laser ablation cluster formation and vapor liquid solid growth was developed and used for the synthesis of ZnO nanostructures. In laser ablation deposition, a laser beam is focused through a vacuum onto the surface of a target material as illustrated in Fig. 2.11. At sufficiently high flux densities and short pulse durations, the target material is rapidly heated to its evaporation temperature and forms a vapor plume. Unlike thermal evaporation, where the vapor composition is dependent on the vapor pressures of the elements within the source material, laser ablation produces a plume of material with similar stoichiometry to that of the target material. Once the vapor plume has been formed, it is collected onto a cooler substrate that promotes nucleation and growth of crystalline films. Sun *et al* [64] reported the synthesis of aligned ZnO nanorod using laser ablation deposition method without using a catalyst.

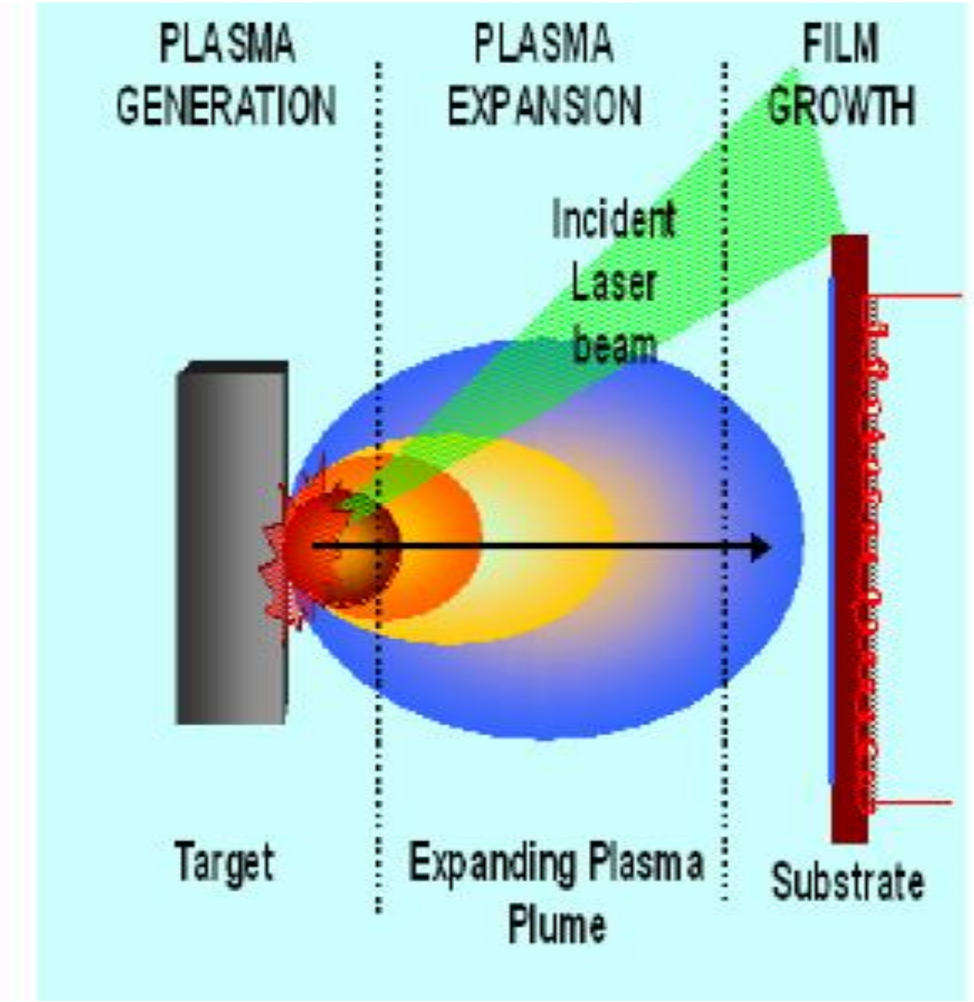

Fig. 2.11. A schematic diagram of pulsed laser deposition (PLD) technique used for ZnO nanofabrication.

2.7.4 Chemical vapor transport and condensation

Chemical vapor transport and condensation (CVTC) is a cheap and effective process for ZnO nanofabrication. Fundamentally, the process is a chemical reaction between the gaseous species at atmospheric pressure. These gaseous species are usually generated by evaporation, reduction, or some other gaseous reaction. The reaction products are transported by carrier gas and then, condense onto the substrate, which is at a lower temperature than the products. Figure 2.12 shows a schematic diagram of a CVTC system for ZnO nanostructures growth. ZnO nanowire growth based on a CVTC process has been reported [4]. Zn vapors in an oxygen ambience had been used. Zinc evaporated over the substrate reacts with oxygen to form ZnO, which then condenses onto the substrate surface. To facilitate the production of ZnO nanowires at a lower temperature, the growth reduction is utilized to decompose high-melting-point ZnO (~1,975° C) into low-melting-point Zn or Zn suboxide (~419° C). The Zn vapor is then transport and deposited on the substrate. Carbothermal reduction approach is one of the most employed techniques to produce Zn vapor. In this approach, graphite is added to pure ZnO powders [58, 59]. At a high source temperature (~1,100° C), Zn or Zn suboxides are produced by the following reactions:

ZnO powder is mixed with graphite powders to form Zn and CO gas as illustrated in Eq. 2.1.

$$ZnO_{(solid)} + C_{(solid)} \rightarrow Zn_{(gas)} + CO \quad \text{------------------} \ (2.1)$$

Then, CO gas worked as reduction agent with ZnO powder to form more of Zn vapor and CO_2 gas as shown in Eq. 2.2.

$ZnO_{(solid)} + CO_{(gas)} \rightarrow Zn_{(gas)} + CO_2$ --------------- (2.2)

Zn and CO_2 vapors were then transported or diffused to a low temperature region (downstream of carrier gas flow), which they reacted to form ZnO/ ZnO_X liquid droplets and CO gas which depart the tube following the reaction shown in Eq. 2.3.

$Zn_{(gas)} + CO_{2(gas)} \rightarrow ZnO_{(\,liquid\,)} + CO_{(gas)}$ -------- (2.3)

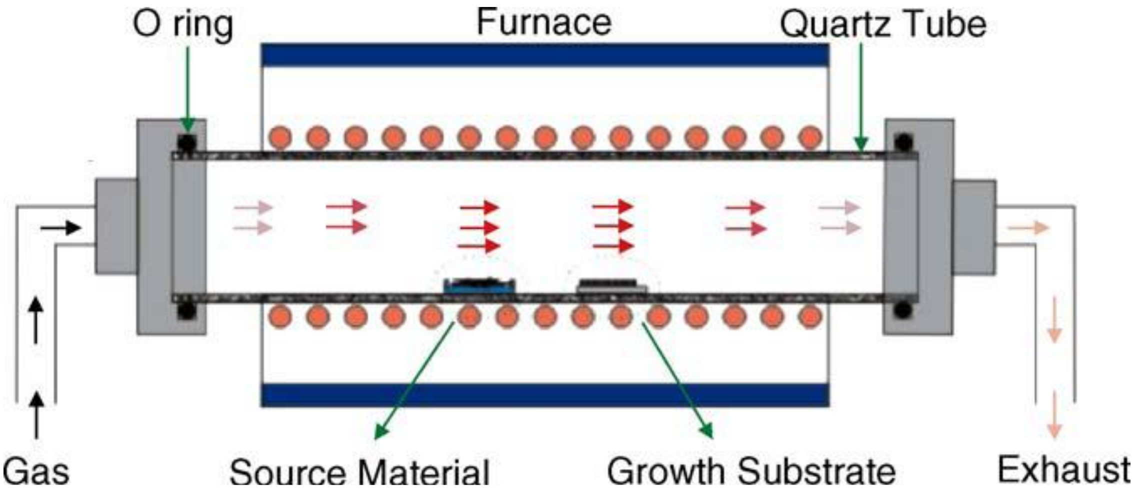

Fig. 2.12. A schematic diagram showing chemical vapor transport and condensation (CVTC) experiment setup [45].

2.7.5 Templates assisted processes

Template-assisted growth is a conceptually simple and straightforward way to synthesize ordered ZnO nanowire arrays. In this technique, a highly ordered nanopore array is formed in a host material, followed by chemical or electrochemical filling of these nanopores using selected materials [65]. Templates can be polymetric filtration membranes or nanoporous alumina films that contain cylindrical holes with diameters down to 4 nm [66]. Anodic alumina oxide membrane (AAO) is the most extensively used templates for nanowire synthesis due to its chemical and thermal stability and high mechanical strength as illustrated in Fig. 2.13 (a). It is prepared via the anodization of pure aluminum in acidic solution [67]. These pores can be filled to form nanostructures using electro-deposition and sol–gel deposition methods as shown in Fig. 2.13 (b).

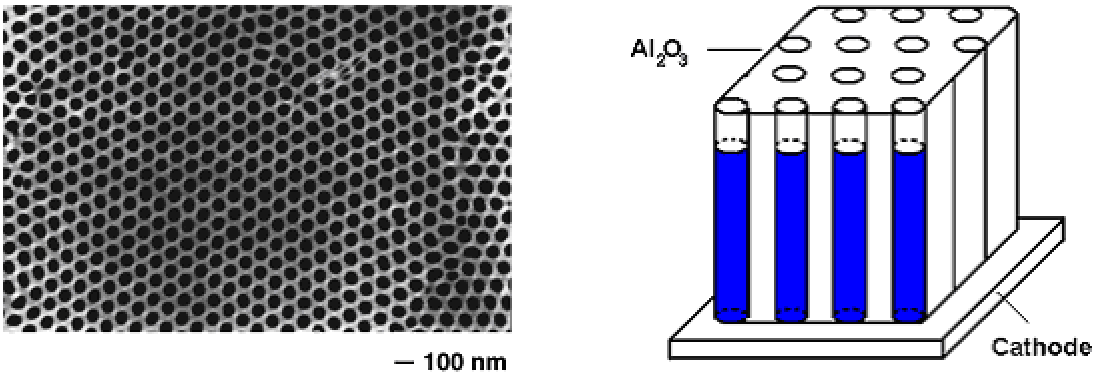

Fig. 2.13. (a) The SEM image of AAO membrane surface and (b) AAO membrane as a template for making ZnO nanowires by electroplating [65].

2.8 Effects of the growth parameters on zinc oxide nanostructures formation

It is worthy to mention that ZnO nanostructures exhibit a wide range of electrical and optical properties that depend sensitively on both shape and size. For that reason, understanding the relationship of different growth parameters and the growth mechanism is very important for controlling the size and shape. The control of the shape and the size of ZnO nanostructures are not easily obtained. Any small change in experimental parameters can be greatly affected the size and shape of the structure. In this section, some of the past studies on the effect of growth parameters on ZnO nanofabrication using chemical vapor transport and condensation (CVTC) growth process using carbothermal reaction will be discussed. The effects of several growth parameters including source material temperature, substrate temperatures, deposition time, gas flow rate, total and partial pressure, substrate material, catalyst species, reaction time and molar ratio of ZnO/C on the growth process will be reviewed.

2.8.1 Source material temperature effect

Source temperature is an important factor in ZnO nanofabrication. Source material temperature indicates the source material vapor pressure. The vapor pressure increases exponentially with the material temperature [68]. High source temperatures will result in more nanostructure growth on the substrates than low source temperatures. The size and shape of the ZnO nanostructures are also affected by the source material temperature. In addition, the source material needs to be hot enough to evaporate and then carried by the flow gas. On the other hand, source vapor nucleates uniformly if a large amount of source material deposits simultaneously on the substrate surface. Chen *et al* [69] used carbothermal route in ZnO nanofabrication and they did not obtain any ZnO nanostructures at source temperature below 900ºC. Zinc oxide powders-like started to form on the substrates at source temperature of 1200ºC. They also reported that the best growth rate and high yield of ZnO nanostructures were optimized at source temperature of 1100ºC. Zhao *et al* [70] stated that the diameters of ZnO nanorods increased as the source materials temperature was increased from 900 to 1000 °C while, the length of these nanostructures decreased. In addition, as the source temperature increased to 1000 °C, ZnO nanosheets had been formed.

2.8.2 Substrate temperature effect

Substrate temperature is one of an important variable for controlling the size and shape of ZnO nanostructures. Li *et al* [71] reported that zinc oxide nanostructures change with substrate temperature. Nano-ridges structures were optioned at the substrate temperature of 900ºC whereas, for the substrate temperature between 790ºC-850ºC, well vertical aligned with high density of zinc oxide nanorods were observed. At 650ºC-750ºC, arrays of nanowall-nanorods junction were found. Moreover, ZnO nano-tips structures were formed at substrate temperature of 550ºC-630ºC. At low temperature region below 550ºC, no ZnO nanostructures had been found and only crystalline films were observed. Umar *et al* [72] also reported different ZnO morphologies as different substrate temperatures. At 470ºC-515ºC substrate zone, pyramidal tower shaped of ZnO nanostructures were observed while, at 515ºC-555ºC, hexagonal faceted ZnO nanorods were reported. In addition, ZnO nanowires attached to nanosheets were obtained at 555ºC-580ºC.

2.8.3 Gas flow rate effect

In fact, there are two main parameters related to in the growth process of the ZnO nanostructures. They are the gas flow rate and gas species. Park et al [73] reported that they could not obtain any ZnO nanostructures when they used only argon gas (without using O_2 gas) at 20 sccm (standard cubic centimeter per minute) flow rate as illustrated in Fig. 2.14.

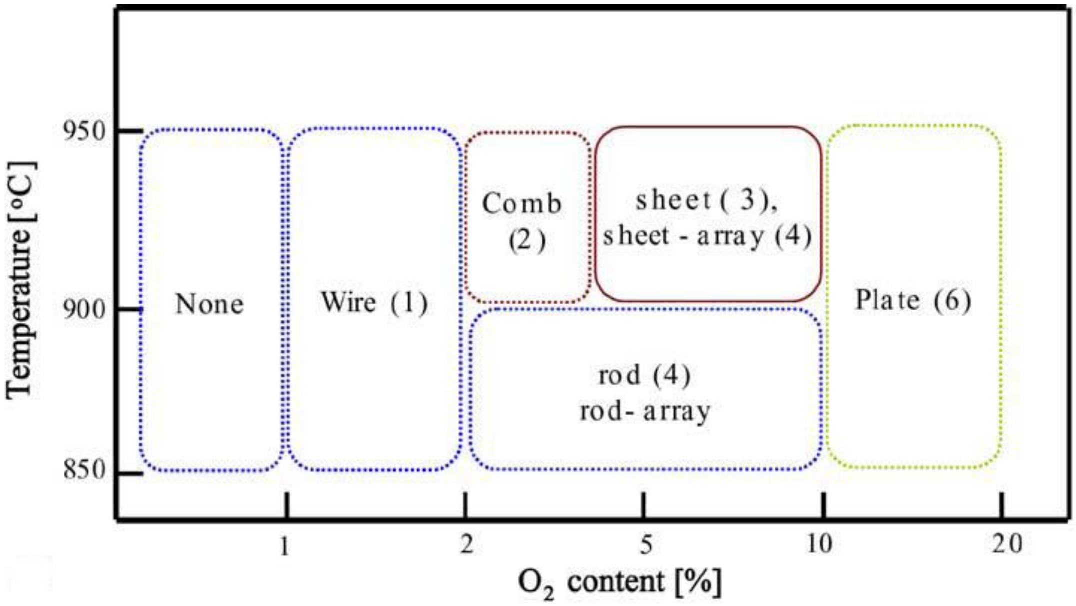

Fig. 2.14. A summarized map of the predominant ZnO nanostructures under certain processing temperatures and oxygen contents [73].

ZnO nanowires began to from on the substrate when they mix more than 0.1% of O_2 with 20 sccm Ar flow rate. When the atomic % of O_2 was increased from 2-20, the ZnO morphology changed from nanowires, nanocomb, nanosheet to nanoplats respectively at substrate temperatures of 850°C-950 °C. Chen *et al* [74] also reported that the ZnO nanostructure morphologies are greatly influenced by the gas flow rate. They used a nitrogen gas as a carrier gas in ZnO nanofabrication using a mixture of ZnO and graphite powders as source materials. They obtained ZnO nano-tetrapod structures were grown on the inner wall of the quartz tube at 70 sccm N_2 flow rate. As the flow rate increased from 90 to 100 sccm, ZnO nanowires were formed instead of nanotetrapods. In contrast, dark-gray color of Zn nanowires were obtained as Nitrogen flow rate increased to 150 sccm. Moreover, Dalal *et al.*[75] reported smaller ZnO nanorods which had a lower areal density and were greater in diameter at lower flow rates and longer nanorods at higher flow rates.

2.8.4 Pressure effect

The gas pressures formed from the source reactions or used in the growth process play an important role on ZnO nanofabrication. Vapor pressure is the key role of zinc oxide supersaturation. Supersaturation is determined by local pressure of the vapors precipitated on the substrate. The vapors pressure of Zn, ZnO_x and CO/CO_2 and the deposition temperatures were gradually decreased from the source materials location to the open side of the tube. Oxygen vapor is essential to allow zinc to deposit on the substrates as zinc oxide, instead of zinc metal. High local oxygen partial pressure will promote (1011) growth of zinc oxide nanostructures [76]. According to this, Yan *et al* [77] made a correlation between the Oxygen partial pressure and the number density of zinc oxide nanorods. When oxygen pressure was equal to 2×10^{-2} Torr, nanorods were grown in high density. If oxygen pressure was lower than 2×10^{-2} Torr, oxygen mainly worked on the substrate surface and leaded to the nucleation of zinc deposited on the substrates. If oxygen pressure was higher than 2×10^{-2} Torr, ZnO nanorod density decreased due to the lack of zinc ions. In addition, Dalal *et al.*[75] reported that the diameter, length, areal density and the morphology of ZnO nanostructures largely change with the deposition pressure as shown in Fig. 2.15. Chen *et al.*[69] demonstrated ZnO nanofabrication at atmospheric pressure without using carrier gas. They reported various ZnO nanostructures; nanowires, nanobelts, and nanofibers formed at different substrates locations under different deposition temperatures and different vapor pressures. In this work, the synthesized ZnO nanostructures at atmospheric pressure has been obtained.

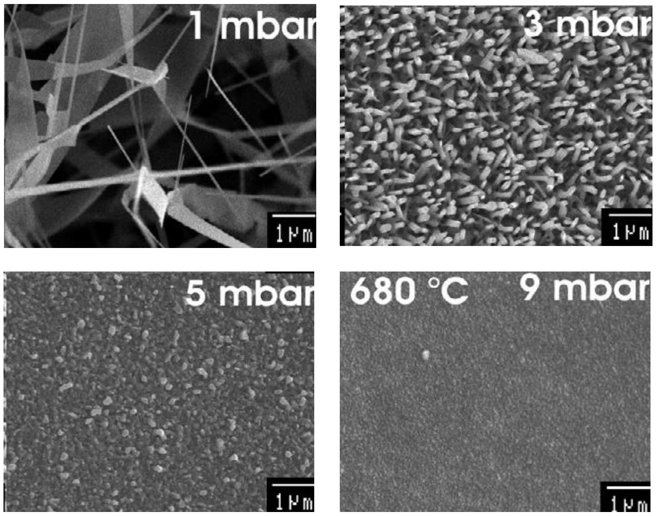

Fig. 2.15. FESEM images of different ZnO nanostructures morphologies obtained at different deposition pressures [75].

2.8.5 Substrate material effect

The substrate material plays a key role in achieving oriented growth of ZnO nanostructures. Various substrates have been utilized for ZnO nanofabrication, including sapphire [78], GaN [79], ZnO coated silicon substrate [80], NiO coated silicon [81], glass [82], Al_2O_3 [83], gold coated silicon [69], SiC [84] and Si [85] *etc*. In most cases, the nanostructures alignments are determined by lattice matching between zinc oxide and the epitaxiy substrates as illustrated in Table 2.3.

Table 2.3. Lattice parameters of several epitaxiy substrates.

Material	ZnO	GaN	Sapphire	SiC	Si
Crystal structure	Wurtzite	Wurtzite	Hexagonal	Wurtzite	Diamond
Lattice constant (nm)	a=0.325 c=0.521	a=0.319 c=0.519	a=0.475 c=1.299	a=0.309 c=1.512	a=b=c =0.543
Epitaxial plane	(0001)	(0001)	(1120)	(0001)	(100)
Lattice Mismatch	0	1.9%	0.08%	5.5%	18.6%

The lattices of these substrates match with zinc oxide in certain crystallographic directions. The ZnO a-axis and the sapphire c-axis have less than 0.08% mismatch, giving rise to a good epitaxial interface between the (0001) ZnO and the(1120) sapphire. Thus ZnO nanowires can be grown vertically on an a-plane (1120) sapphire substrate. GaN could be an even better candidate because it has the same crystal structure and similar lattice constants to that of ZnO. Fan *et al* [86] confirmed this argument. They used sapphire a-plane and GaN (0001) plane as epitaxy layer for ZnO nanowire growth. They concluded that ZnO nanowires grown on GaN show better vertical alignment than those grown on sapphire substrates. Moreover, ZnO matches with itself very well as can be seen from Table 2.3.

2.8.6 Catalyst effect

Catalysts are playing very important roles in vapor deposition method including; initiates, guides, controlling orientations, alignments, diameters and precise locations of ZnO nanostructures. The metal catalyst can be rationally chosen from the phase diagram by identifying metals in which the nanostructure components are soluble in the liquid phase but do not form solid compounds that are more stable than the desired nanowire phase. Various catalysts have been used and achieved similar results such as Au [87], Co [88], Cu [89], NiO [90], Sn [91], and Au/Pt [92], *etc*. ZnO nanostructures growth requires a few hours of preannealing if catalyst has been predeposited on the surface. Preannealing of the catalyst causes the formation of small catalyst islands, which act as the nucleation centers for the subsequent growth of ZnO nanostructures. The size of the ZnO nanowires obtained depends greatly on the size (diameter and thickness) of these catalyst islands [93]. These catalyst islands work as preferred sites to attract the vapors that formed from carbothermal reaction to form alloy droplet followed by the nucleation and growth of solid ZnO nanowire due to the supersaturation of the liquid droplet. Continuous growth of the nanostructures taking place at the droplet interface constantly pushes the catalyst upwards. Figure 2.16 shows a Transmission Electron Microscopy (TEM) image of a ZnO nanowire terminated with an alloy droplet [94].

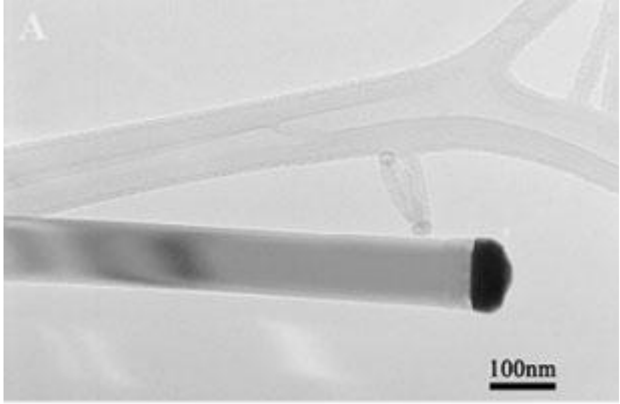

Fig. 2.16. TEM image of a ZnO nanowire terminated with an alloy droplet [94].

Andreazza-Vignolle *et al*.[93] studied the effect of gold and platinum catalysts in ZnO nanofabrication. In the case of gold catalyst, ZnO nanorods were obtained with (001) preferential growth direction whereas, ZnO nanoribbons with preferential (100) growth direction were obtained when platinum had been used as a catalyst. They concluded that the nature and size of the catalyst had a significant effect on the morphology of ZnO nanostructures. In addition, the thickness of the catalyst layer was found to be an important factor determining the size of ZnO nanostructures [4].

2.8.7 Deposition time effect

There are only few reports on the effect of the deposition time on the growth process of ZnO nanostructures. Park *et al*.[95] studied the effect of growth time on morphologies of ZnO nanostructures and they reported different ZnO morphologies at different deposition time. ZnO nanowires were obtained at very short deposition time. As the reaction time increased, dendritic side-branch nanowires started to grow, resulting in highly defined and aligned comb-like architectures. With further time increment, the side-branches continued to grow and planar filling of the interspaces between the evenly spaced side-branches proceeded, eventually resulting in an ultrawide nanosheet as can be seen in Fig. 2.17. On the other hand, Tak *et al*.[96] found that as the reaction time increased, the density of ZnO nanorods/ nanodots was increased and they produced a high density of ZnO nanostructures at long deposition time.

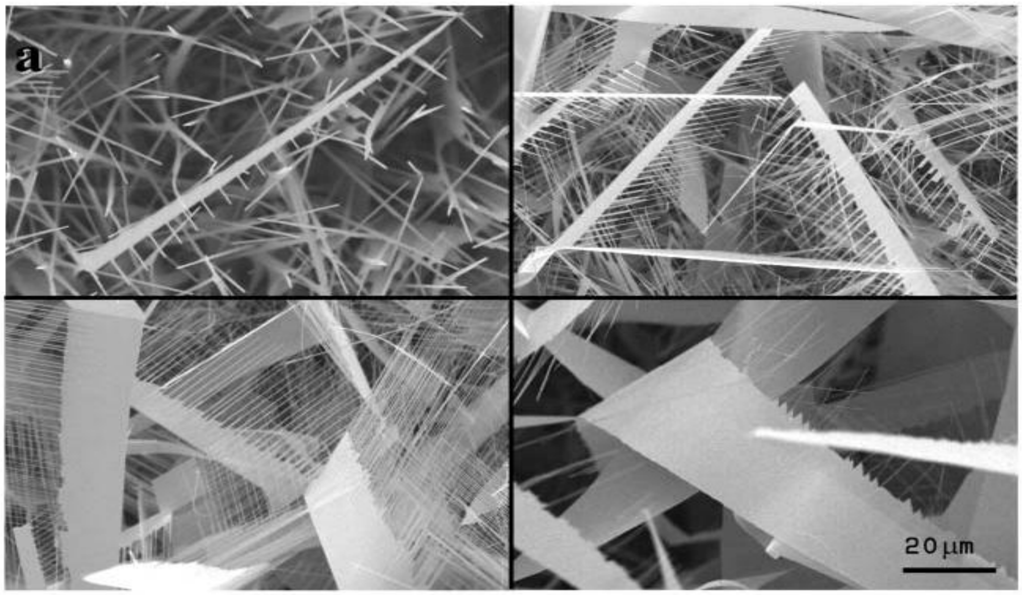

Fig. 2.17. SEM images showing the evolutionary stages of the nanosheets from the comb-like structures toward the sheet structures that were obtained by controlling the growth time from a few seconds to several hours [95].

2.8.8 Mass ratio of ZnO:C effect

As it was mentioned above, ZnO powder is mixed with graphite powder as source material in carbothermal method in ZnO nanofabrication. The advantages of this method is that the existence of graphite significantly lowers the decomposition temperature of ZnO powder. Chen *et al*. [69] reported that they could not obtained ZnO nanostructures by heating ZnO powder without carbon powder at sintering temperature of 1100°C. They also reported that fewer of ZnO products were obtained when a small quantity of carbon powder was mixed with ZnO powder as reactants, when excess carbon powders were added into the reactants, the growth rates became faster and the wires were longer. They concluded that the growth rates and the resultant yield of ZnO nanostructures were mainly influenced by the quantity of the carbon powders. In another study, Lim *et al*.[97] used graphite and three kinds of carbon black powder as source materials for the carbothermal reduction. They studied the effects of carbon surface area on the carbothermal reaction. Three kinds of carbon black powder with different surface areas equal to 70, 236 and 1440 m^2/g had been mixed with ZnO powder. They reported that the growth rate of ZnO nanostructures was strongly dependent on the surface area of carbon source. In other words, the fabrication of ZnO nanostructure could be performed more efficiently by using carbon source with a large surface area. Their result agreed with Leung *et al.*[98] who found that the carbothermal reduction for ZnO nanostructure fabrication could be significantly enhanced by using single-walled carbon nanotube.

2.9 Growth mechanism of ZnO nanostrctures

Several growth mechanisms have been established to illustrate the growth process of ZnO nanostructures. In this section, various mechanisms that have been used in ZnO nanofabrication field will be illustrated in details.

2.9.1 Vapor-liquid-solid

The vapor-liquid-solid (VLS) mechanism is well established and most widely accepted. It was proposed by Wagner and Ellis in 1964 to explain the growth of Si whiskers using Au as a metal catalyst [99]. The key point in the process is that metal catalysts like Au, Ni, Co, Fe, get involved in the experiment. According to VLS mechanism, it consists of three stages which are illustrated in Fig. 2.18. In the first step, a metal particle absorbs semiconductor material and forms alloy. In this step the volume of the particle increases and the particle often transitions from a solid to a liquid state. In the second step, the alloy particles absorb more semiconductor material until it is saturated. The saturated alloy droplets are in equilibrium with the solid phase of the semiconductor and nucleation occurs. During the final phase, a steady state is formed in which a semiconductor crystal grows at the solid/liquid interface. The precipitated semiconductor material grows as a wire because it is energetically more favorable than extension of the solid/liquid interface. Due to the much larger accommodation coefficient of the reactants in the liquid, the growth rate is much faster at the solid/ liquid interface compared to the solid/ vapor interface [100].

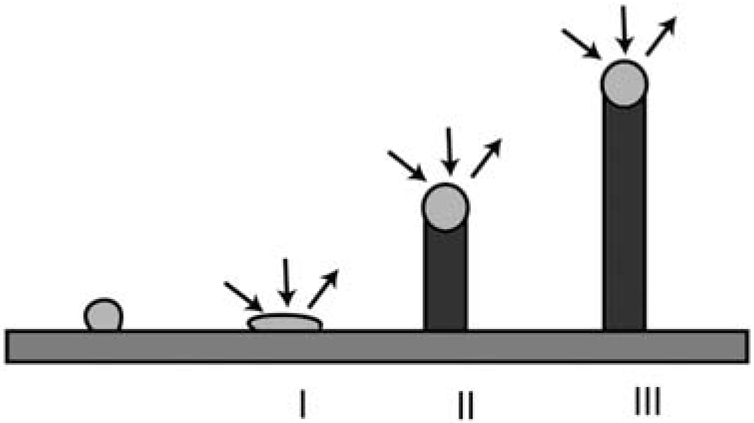

Fig. 2.18. VLS diagram process consists primarily of three steps: (I) formation of the liquid alloy droplet, (II) crystal nucleation upon gas adsorption and supersaturation, and (III) axial growth from the crystalline seeds to form nanowires [101].

In the VLS mechanism, the wire diameter is determined by the diameter of the alloy particle which is in turn determined by the size of metal particle and temperature. The wire length is determined by the growth rate and the deposition time [102]. When the system is cooled, the alloy droplet solidifies at the wire tip. According to VLS theory, the catalyst must be selected to ensure that it will exist in the liquid phase above the vapor/metal eutectic point at the experimental temperature and pressure. This ideal catalyst, should not chemically react with the vapor species but should be allowed to diffusion into the droplet and physical alloying of source vapors with the metal liquid. Gold (Au) is a commonly chosen catalyst in the semiconductor and oxide nanowire syntheses due to its low melting point, tendency to form spherical droplets on common substrates, and noble chemical nature in bulk. To find an eligible metal, the phase diagram is first consulted. A material that forms a liquid alloy with the nanowire material of interest is chosen. The phase diagram is also helpful for estimating the optimal composition and temperature for nanowire growth. Figure 2.19 shows a binary phase diagram of gold suitable for VLS assisted growth of nanowires. According to Fig. 2.19, the growth of ZnO nanowires can be done by using Au clusters as a solvent at high temperature and silicon as a substrate. Si and Au form a liquid alloy when the temperature is higher than the eutectic point (363 °C) at stage I. The liquid surface has a large accommodation coefficient and it is a preferred deposition site for the incoming Zn and O_2 vapors. After the liquid alloy becomes supersaturated with ZnO, precipitation of the ZnO nanowire occurs at the solid-liquid interface (stages II–III). For Au catalyzed ZnO nanowire growth, Au nanoparticles were not only observed at the tip [103] of the wires, which is typical for Au catalyzed semiconductor nanowire growth, but sometimes also at the root [104] of wires after growth.

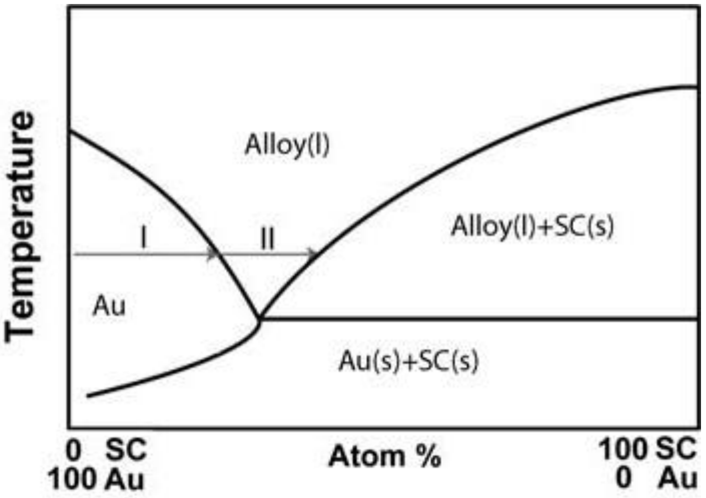

Fig. 2.19. Pseudobinary phases of gold when a gold droplet absorbs semiconductor material at a constant temperature.

The diameter of a nanowire via VLS growth is primarily determined by the liquid alloy droplet, and the thermodynamic-limited minimum radius is given by Eq. 2.4 [4]:

$$\mathbf{R_{min}=2\sigma_{LV}\,V_L/RT\,ln}\mathit{s} \qquad (2.4)$$

Where σ_{LV} is the liquid/ vapor surface free energy, V_L is the molar volume of liquid, and *s* is the vapor phase supersaturation.

2.9.2 Self catalytic vapor-liquid-solid

Self catalytic vapor-liquid-solid **(**VLS) growth mechanism was reported by Dang *et al.* [105] which has no external catalyst introduced into the VLS growth of 1D nanostructure. By a real-time in situ observation of the GaN nanowires growth from Ga liquid droplets, Yang's group gave a strong support to self catalytic VLS mechanism [101]. They demonstrated that Ga droplets function as preferred deposition site for the incoming vapors during the fabrication process. They also reported that the self-catalytic VLS process is provided a promising approach to synthesize pure nanostructures. In addition, Yang's group did not observe any tip particles at the ends of the nanowires. In ZnO growth mechanism, Zn/ZnO or Zn/ZnO_X liquid droplets function as catalysts during the growth process. Zn vapor can be generated by the reduction of ZnO powder by carbon at the high temperature region. Then, the Zn vapor can be transported or diffused to a low temperature region (downstream or upstream of carrier gas flow), where a part of Zn vapors is condensed on the substrate to form liquid droplets. These droplets are preferred sites to absorb ZnO or ZnO_X vapor species. It means that the Zn/ZnO or Zn/ZnO_X liquid droplets have a high accommodation coefficient and function as a nucleation site for subsequent Zn and Zn-suboxides. The vapor components are absorbed by the alloy droplet until it become supersaturated then, the nucleation are occurd. Furthermore, CO/CO_2 gases that form from the carbothermal redaction are reacted with Zn/ZnO_x droplets to form ZnO nanocrystals as illustrated in Fig. 2.20.

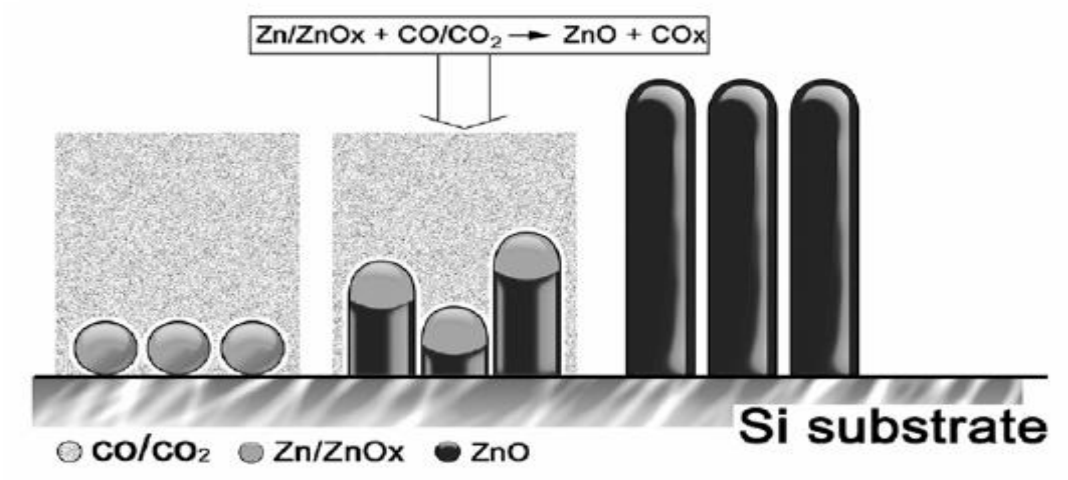

Fig. 2.20. The growth of the ZnO nanowire by a self-catalytic VLS process.

2.9.3 Vapor-solid

In 1950s, G. W. Sears proposed a vapor-solid (VS)-based whisker growth model [106]. It is a commonly observed phenomenon and it is also a catalyst-free process that forms 1D nanostructure. In this process, the evaporation and chemical reduction reaction generates the vapor. Then, the vapor is subsequently transported and condensed on the substrate as shown in Fig. 2.21. The VS mechanism has been used to explain the growth of ZnO nanostructures. Kong *et al* [107] explained that ZnO powder was decomposed into Zn^{2+} and O^{2-} at ~1350 °C and under Ar carrier gas. In their study, nanohelixes and nanobelts were synthesized ono an alumina substrate at a low temperature zone (400-500 °C).

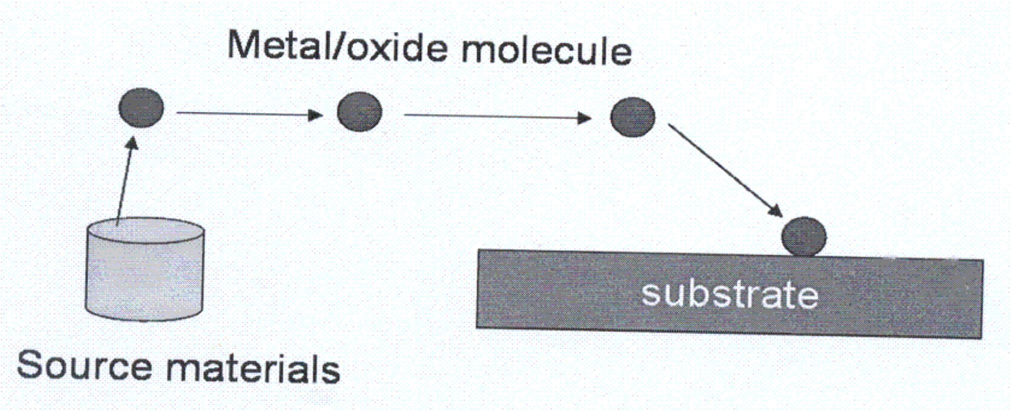

Fig. 2.21. A schematic diagram illustrating the formation of metal oxide nanostructures directly by the vapor solid mechanism on the substrate.

Dai *et. al.* [108] developed a conceptual model to explain the VS growth of ZnO nanobelts. The growth process according to VS route is summarized as shown in Fig. 2.22. ZnO vapor molecules are released from the solid state at elevated temperatures and are condensed on the substrate which is located in a cooler region of the furnace (Fig. 2.22 (A)). As more addition molecules are arrived, a critical nucleus is developed (Fig. 2.22 (B)) and continued to grow with each adsorbed molecule (Fig. 2.22 (C)). According to this process, the local vapor supersaturation remains constant through the pressure control within the furnace. As a consequence of the relatively high mobility of the molecules at the deposition temperature (~800ºC), the molecules are migrated to the high-energy growth front during the formation of series of steps (Fig. 2.22 (D)). The rough tip surface becomes an energy sink for incoming vapor molecules resulting in the rapid formation of ZnO nanobelt (Fig. 2.22 (E)).

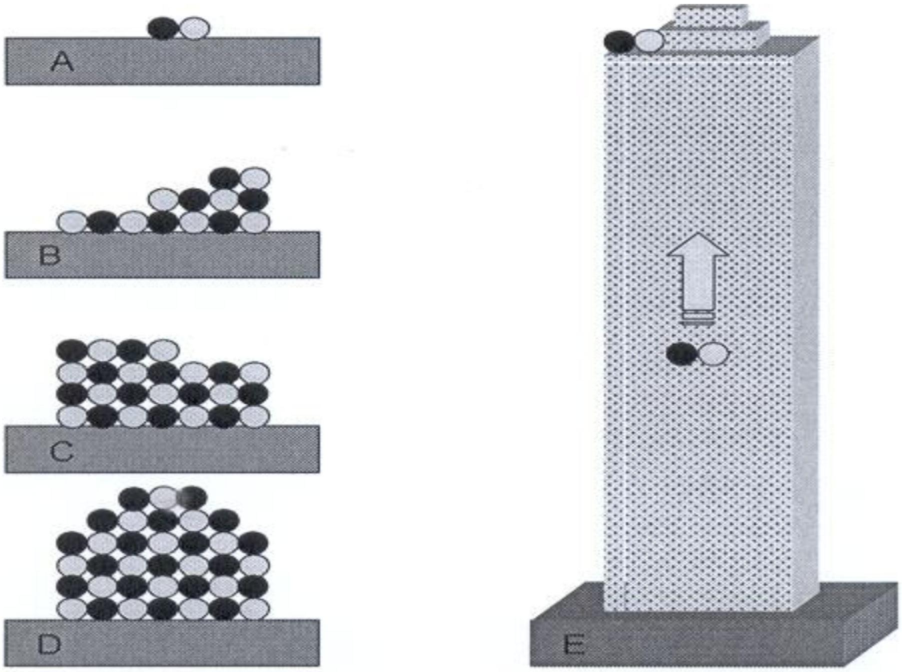

Fig. 2.22. A schematic diagram of proposed growth mechanism for ZnO nanobelts through a VS process [108].

In addition, dendritic ZnO nanowires with abruptly narrowed sharp tips are formed during VS growth. According to Zhang *et. al.* [109] study, the atoms are impinged onto the whisker side surface, adsorbed onto the surface, and diffused along the lateral surface into an atomic sink at the tip of the whisker. Those atoms not reaching the tip are removed by re-evaporation because of their unstable energies. As a result, the crystal growth occurs at the tip of the nanowire. The enormous atomic sink exists for sequential growth, whereas the growth is a diffusion-limited process. As a result, VS process provides less control on the geometry, alignment and precise location of ZnO nanostructures.

2.9.4 Vapor-solid-solid

Vapor-solid-solid (VSS) Mechanism was proposed by Persson *et al.* [110] for the GaAs nanostructures growth using gold partials as a catalyst. Based on results, they reported that the solid phase diffusion was observed by in situ during the synthesis of nanowire. Later, Dick *et al.* [111] found that VSS growth mechanism was also applicable for the gold catalyzed III-V semiconductor nanowires synthesis. Recently, Kirkham *et al.*[112] reported that solid gold nanoparticles play as catalyst for growing aligned ZnO nanowires. The VSS happened when the formation of nanostructures on metal nanocluster catalyst at temperatures below the eutectic. According to VSS, the nanoparticles having diameters much larger than those formed at melting temperature as shown in Fig. 2.23. In ZnO nanowire Au-catalytic growth, the growth has been reported at 500 ◦C, which is almost 200 ◦C below the Au–Zn eutectic temperature (684 ◦C) [113].In addition, the growth mechanism of InAs nanowires was also attributed to VSS process. It has been proposed that the catalyst particle can be found in a solid state during growth process [114].

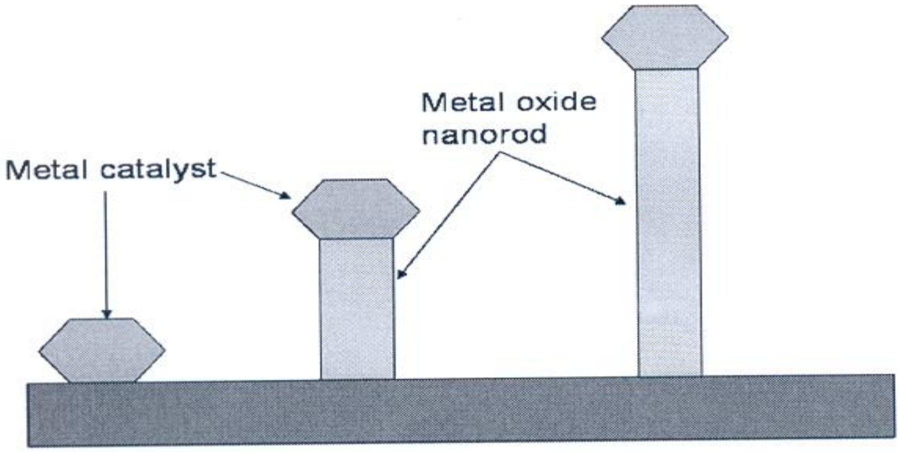

Fig. 2.23. A schematic diagram illustrating the formation of metal oxide nanowires via vapor-solid- solid mechanism.

2.10 Characterization techniques

The deposited products were characterized by field emission scanning electron microscopy (FESEM, Quanta 200F), energy dispersive x-ray spectroscopy (EDX) spectrum (Oxford Inst), and x-ray diffraction (XRD, Siemens D-5000 diffractometer by using copper-monochromatized Cu Kα1 radiation (λ=1.540598 Å) under the accelerating voltage of 40 kV and the current of 40 mA with a normal 2θ scan. Conventional TEM analysis and high-resolution transmission electron microscope (HRTEM) were both performed on a JEOL-2010 microscope at 10–200 kV. In addition, the optical properties of the grown ZnO nanostructures samples were characterized by photoluminescence (PL). PL measurements were performed at room temperature by using a Jobin Yvon Horiba HR800UV system. In this system, a He-Cd laser (325 nm) was used as an excitation source with a power of 20 mW.

2.10.1 Field emission scanning electron microscopy

The field emission scanning electron microscopy (FESEM) uses electrons instead of light to form an image as shown in Fig. 2.24. The electron beam has a much smaller wavelength than the white light which allows the resolution of the surface detailed down to sub-micrometer levels. A beam of electrons is produced at the top of the microscope by field emitted by a cathode filament (WorLaB_6) or a filed emission gun (W-tip). The electron beam follows a vertical path through the column of the microscope. It makes it’s away through electrostatic condenser lenses which focus and direct the beam downwards to the sample. When the beam hits the sample, other electrons are ejected from the sample. These ejected electrons are called secondary electrons. Secondary electrons have a low energy and can escape only from a very thin layer of the surface. The main effective area of secondary electron emission is very close to the specimen-incident beam interface. Therefore, the probe size is the dominant feature in the resolution capability of the FESEM. Detectors are collected the secondary electrons and covert them into a picture of the surface on either a viewing screen or a micrograph. If the sample is transparent, the primary beam penetrates the surface and produces a variety of signals which can be used to generate micrographs. The specimen-beam interaction also produces backscattered electrons (these are elastically scattered electrons), Auger electrons and x-ray. X-ray can be used to qualitatively and quantitatively analyze the elemental composition and distribution in the sample. In addition, the induced current can be developed in smi-conductive specimens. These signals are used to produce images (micrographs) of the surface [115]. The different signals that can be produced by FESEM are shown in Fig. 2.25.

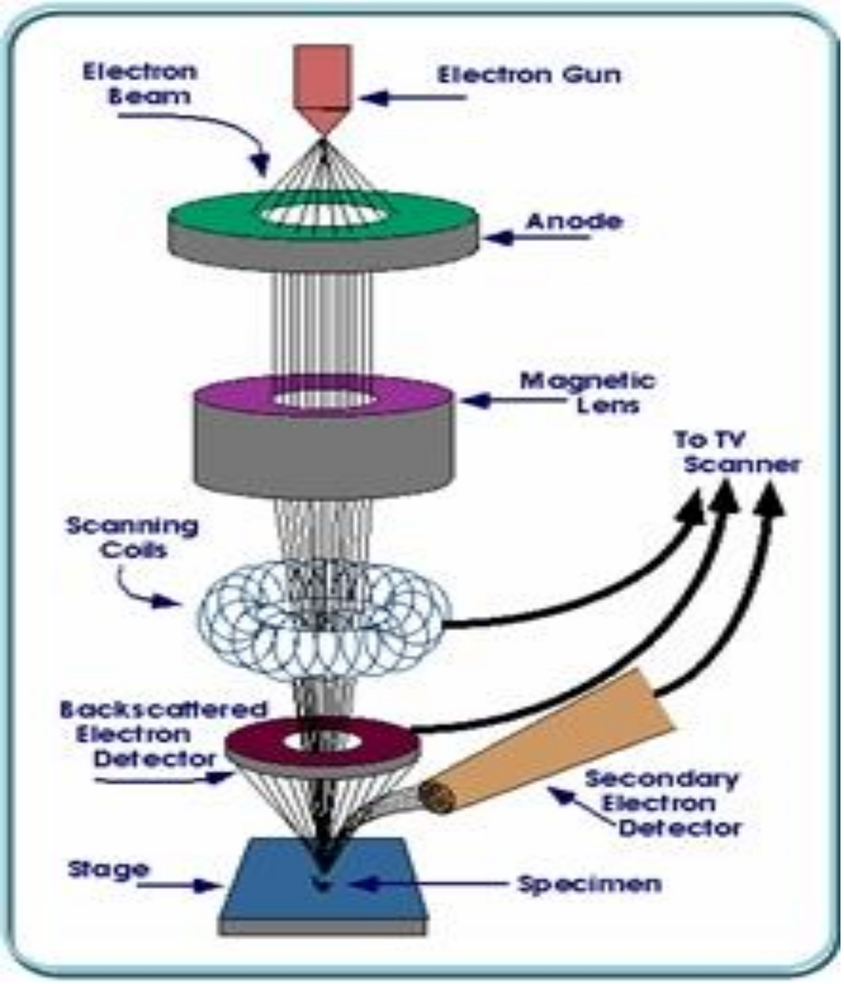

Fig. 2.24. A schematic diagram illustrating the function principle of the FESEM.

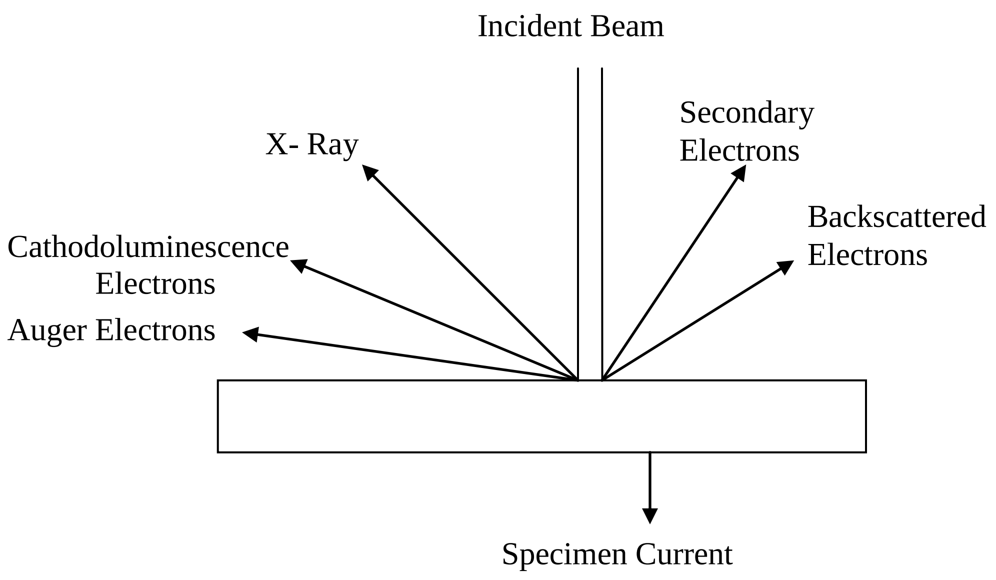

Fig. 2.25. Some of the signals which used in FESEM.

SEM setup

The experimental setup consists of an electron gun, column, scanning system, substrate chamber and detectors.

Electron gun

Electron gun is based on the thermal emission. The electron source is commonly a tungsten (W) or lanthanum hexaboride (LaB6) tip. Electrons are emitted from the cathode during heating process.

Column

The column consists of two electromagnetic lenses acting on the electron beam. The first lens, the condenser lens, produces most of the beam demagnification. The second lens, objective lens, focuses the beam onto the sample. In the column, a beam shaper called stigmator, the stigmator can create a magnetic field around the beam to restore it in a circular cross section.

Scanning system

To get an image on the display, the beam should be scanned over the specimen and the displayed tube. Information from any point on the sample are reproduced in the same relative position on the display.

Substrate chamber

The substrate holder depends on the different size and shape of the sample. The sample can be moved in three dimensions, as well as rotated and titled.

Detector

Scintillation detectors mostly used in FESEM. They can be used for primary electrons.

X-ray detector

Spectrometers for detection and analysis of x-ray are based on either of two principles;

- Wavelength dispersive x-ray (WDX); determines the wavelength of the x-rays.

- Energy dispersive x-ray (EDX); determine the energy of the x-rays.

2.10.2 Transmission electron microscopy

Transmission electron microscopy (TEM) is an invaluable analysis technique for nanostructure materials because of its ability to offer a physical image, chemical information through spectroscopic techniques, and crystallographic information via electron diffraction patterns. A TEM is in many ways similar to a light optical microscope. Both types are built up with a clarification and an image part, where the first illuminates the sample and the second focus the beam to the detector. In TEM, electrons instead of photons are irradiating the sample. Since electron scatters very quickly in air, the beam pathway including the sample has to be under vacuum. Moreover, electromagnetic lenses are used to bend the electron beams. Electrons are accelerated with 200 kV correspond to a wavelength (λ) of 2.5 pm, which is several orders smaller than for visible light (~400-750 nm), the result is greater resolution. The electrons in TEM are accelerated by typically a few hundred kV and directed through an electron transparent specimen. The electrons interact with the sample and are scattered in different ways depending on the structure of the sample. Subsequently, the scattered electrons will arrive at a detector, usually a fluorescent screen, CCD camera or an analogue camera, where the image is obtained as shown in Fig. 2.26.

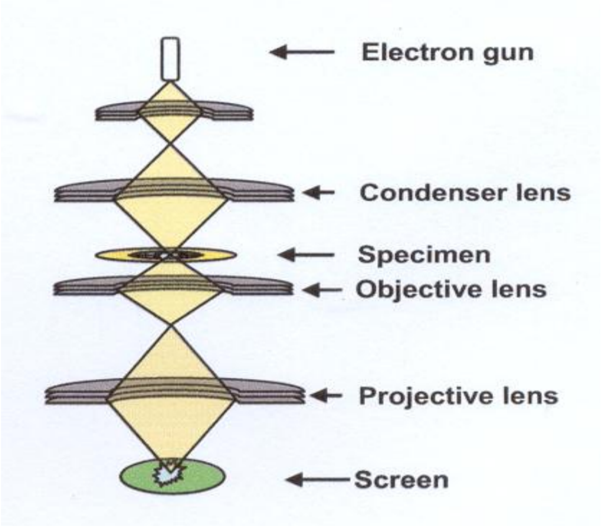

Fig. 2.26. A schematic diagram illustrating the function principle of TEM.

In order to study crystallographic information from a definite area, a selected area aperture can be introduced, which blocks the beam of electrons from reaching other divisions of the sample. This is called selected area electron diffraction (SAED). To obtain a TEM image, the electron beam must interact with the sample and give contrast. When the electrons arrive at the sample they can either be transmitted, absorbed, scattered or backscattered. If all scattered and transmitted electrons are reached the image plane, the resulting image will typically have little contrast (Fig. 2.27. (a)). To defeat this, an aperture can be introduced in the back focal plane of the objective lens where the diffraction pattern is built up as spots to block parts or all of the diffracted beams and thus obtain bright-field diffraction imaging (Fig. 2.27. (b)). In contrast, dark-field diffraction imaging is obtained by blocking all spots except one or more diffracted spots (Fig. 2.27. (c)).

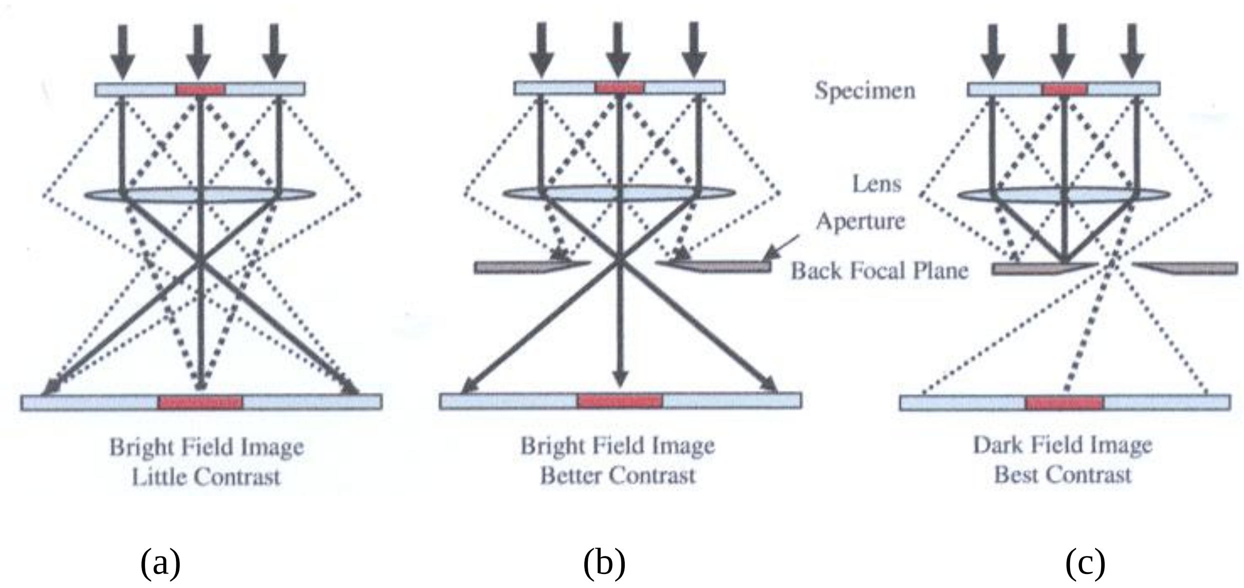

Fig. 2.27. Three examples of imaging modes; (a) bright field mode with transmitted plus diffracted beam with little contrast, (b) bright field mode with only transmitted beam with better contrast since the diffracted beam is blocked and (c) dark field mode where only the diffracted beam is used.

2.10.3 X - ray diffraction

X-ray diffraction (XRD) is a versatile, non-destructive technique used for qualitative and quantitative analysis of a crystalline materials. This experimental technique has been used to determine the overall structure of bulk solids, including lattice constants, identification of unknown materials, orientation of single crystals, orientation of polycrystalline, stress, texture, grain size, etc.

2.10.3.1 Generation of x- ray

X-rays are short-wavelength, high energy electromagnetic radiation, having the properties of both waves and particles. They can be described in terms of both photon energy (E) or wavelength, λ (the distance between peaks) and frequency ν (the number of peaks passing a point in a unit of time). The relation between energy, frequency or wavelength in the case of photon is presented in Eq. 2.5:

$$E = h\,\nu \qquad (2.5)$$

The X-ray cab be produced when electrons of high energy strike a heavy metal target, like tungsten or copper. When electrons hit this material, some of the electrons will approach the nucleus of the metal atoms where they are deflected because of there opposite charges (electrons are negative and the nucleus is positive, so the electrons are attracted to the nucleus). This deflection causes the energy of the electron to decrease, and this decrease in energy results in forming an x-ray. Continuum x-rays are produced when incident beam electrons are slowed to varying degrees by the strong electromagnetic field of atomic nuclei in the sample. All degrees of electron braking are possible and, thus, the resulting x-rays have a continuous range of all energies. Each incident electron potentially can undergo many such interactions in a solid. Continuum radiation is also called bremsstrahlung, German for "braking radiation". X-ray spectrum with a Bremsstrahlung background is shown in Fig. 2.28. The electrons which are stopped in just one impact producing photons of maximum energy equal to the energy loss [117].

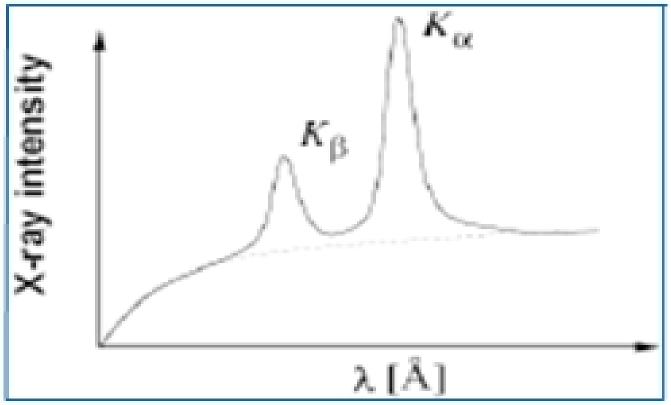

Fig. 2.28. X-ray spectrum with a Bremsstrahlung background and electrons excitations.

2.10.3.2. Bragg’s law

Since atoms are arranged periodically in a lattice, x-rays scattered from a crystalline solid can constructively interfere, producing a diffracted beam through these atoms as it illustrated in Fig. 2.29. In 1912, W. L. Bragg recognized a predictable relationship among several factors. These factors are combined in Bragg’s law as in Eq. 2.6 :

$$n\lambda = 2d\sin\theta \qquad (2.6)$$

Where, n = an interger 1, 2, 3….etc, λ = the wavelength of the incident x-radiation, symbolized by the Greek letter lambda and, in this work, is equal to 1.54 angstroms, d = the distance between similar atomic planes in a mineral (the interatomic spacing) which it is called the d-spacing and θ = the diffraction angle in degree.

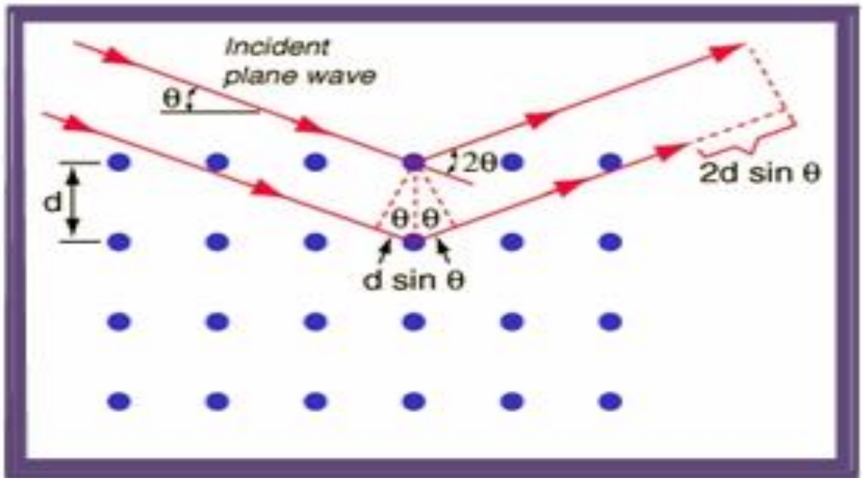

Fig. 2.29. Bragg's diffraction condition.

2.10.4 Photoluminescence measurements

Photoluminescence (PL) is the spontaneous emission of light from a material under optical excitation. The excitation energy and intensity can be chosen to investigate different excitation types and also different parts of the sample. (PL) is used as characterization technique of semiconductor physics for a number of reasons [117,118]. First, PL analysis is nondestructive because it is based on pure optical processes. Second, it requires very little sample preparation or environmental control. Third, it is very sensitive technique. In fact, PL investigations can be used to characterize a variety of materials parameters such as the size of the band gap, impurity levels, recombination mechanisms and material quality. In the typical process, when light of enough energy is illuminated a material, photons are absorbed and (electronic) excitations are created. These excitations relax and produce a photon. In addition, the excitation energy is kept fixed, while the detection energy is scanned. The emitted luminescence is collected, and intensity is recorded as a function of the emitted photon energy, to produce a PL spectrum. The PL spectrum reveals transition energies and the PL intensity gives a measure of the relative rates of radiative and non-radiative recombination. The energy of emitted photon is characteristic for radiative recombination process.

2. 10. 4. 1 Radiative recombination mechanisms observed in PL

In semiconductors, the luminescence can be achieved by several radiative transitions between the conducation band and valence band, exciton, donor and acceptor levels, as it shown in Fig. 2.30. Upon excitation at energy above the bang gap, free electrons are created in the conduction band together with the free holes in the valence bond. These carriers will energetically relax down the band edge. Due to mutual coulomb interaction, electron-hole pair is formed. This electron-hole usually called a free exciton (FE). Its energy is slightly smaller than the bang gap energy. This energy difference is the binding energy of the free exciton. A neutral donor (acceptor) will give rise to an attractive potential, a free exciton might be captured at the acceptor (donor) and abound exciton (BE) is formed. An electron bound to a donor can recombine directly with a free hole from a valence band. This kind of recombination is called free-to-bound (FB) transition. The recombination energy for such a transition corresponds to the band gap energy reduced with the binding energy of donor. Another possibility is that a hole bound to an acceptor recombines with an electron bound to a donor in donor-acceptor pair (DAP) transition. Both the donor and the acceptor are neutral before the recombination (i.e. the donor positively and the acceptor negatively charged). Thus there is a Coulomb interaction between the donor and acceptor after the transition and extra Coulomb energy is gained in the final state added to the radiative recombination energy. The transition energy depends on the distance R between the donor and acceptor atoms.

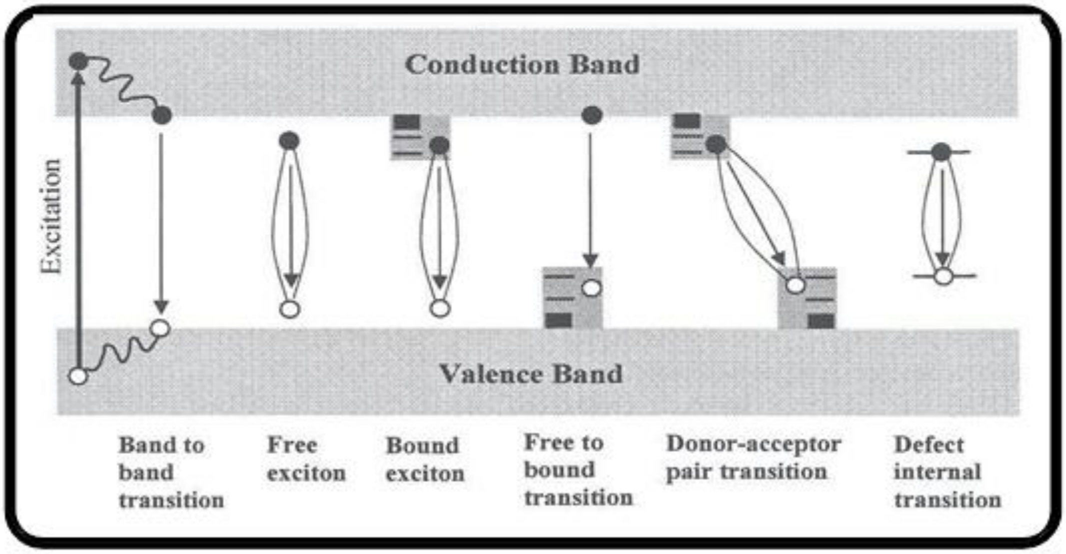

Fig. 2.30. A schematic diagram illustrating of common recombination processes [119].

2.10.4.2 Micro- photoluminescence spectroscopy

High spatial resolution is gained in the micro-PL by replacing the lens focusing the laser on the sample by a microscope objective. The microscope objective offers the possibility to focus the laser spot down to 2μm in diameter and gives the value up to μm- precision in the sample position. The focusing of the light is managed by moving the objective, while the cryostat, which makes possible measurement at very low temperature, is adjusted vertically and horizontally to change the position of the excitation spot. A magnified image of the sample is taken from the CCD-chip of a video camera, allowing precise control of laser focusing and sample position.

2.10.4.3 Experimental setup

The experimental setup consists of an excitation source, microscope objective, monochromator, CCd-TV camera and additional components as illustrated in Fig. 2.31 [119].

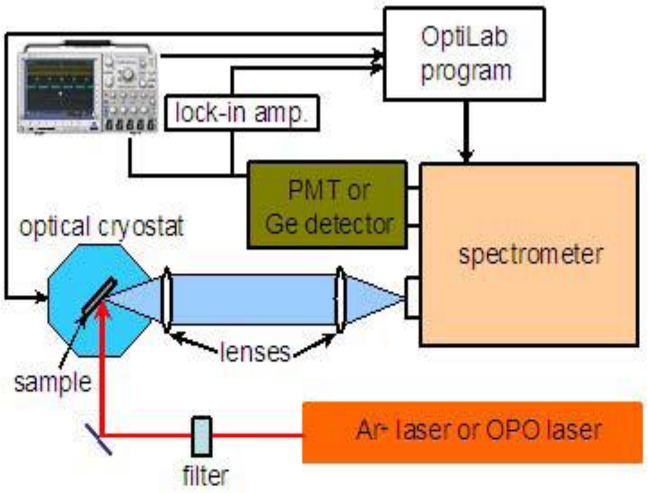

Fig. 2.31. A schematic diagram illustrating the PL system.

Excitation source

Excitation source is usually a laser, which provides a stable and well defined source of the monochromatic light.

Microscope objectives

The microscope objective, outside the cryostat is used for both by focusing laser light excite and collect the emitted light from the sample. By using beam splitters and mirrors the collected light is guided to spectrometer and detector.

Monochromator

The monochromator was used to choose wavelength that will reach the detector at the exit of silt of the monchromator.

Video camera

Video camera is used for obtaining an image of the surface on the monitor. This is achieved by illuminating the sample with white light lamp through the microscope objective and detecting light from the sample. The camera helps to see location of the sample and guaranties. The camera also shows the laser spot and helping in obtaining the optimal alignment of the setup.